A PROPOSED MODEL FOR RENAL BLOOD FLOW CONTROL

Thesis for the Degree of Ph. D.
MICHIGAN STATE UNIVERSITY
CLYDE R. REPLOGLE
1967

This is to certify that the

thesis entitled

A Proposed Model for Renal Blood Flow Control

presented by

Clyde R. Replogle

has been accepted towards fulfillment
of the requirements for

Ph.D. degree in Physiology

W. D. Collings
Major professor

Date July 28, 1967

A PROPOSED MODEL FOR RENAL BLOOD FLOW CONTROL

By

Clyde R. Replogle

AN ABSTRACT OF A THESIS

Submitted to
Michigan State University
in partial fulfillment of the requirements
for the degree of

DOCTOR OF PHILOSOPHY

Department of Physiology

1967

ABSTRACT

A PROPOSED MODEL FOR RENAL BLOOD FLOW CONTROL

by Clyde R. Replogle

Autoregulation of blood flow in the kidney was recognized by Rein in 1931, and its characteristics have been described by many authors (Hartmann, et al. 1936; Forster and Maes, 1947; Selkurt, 1946; Hinshaw, et al. 1959; Scott, et al. 1965). Although there are few arguments over the existence of and the description of renal autoregulation, there have been many hypotheses attempting to explain the mechanism of its operation (Harvey, 1964; Scott, et al. 1965; Haddy and Scott, 1965; Hinshaw, 1964; Replogle 1960a; Schmid and Spencer, 1962; Waugh and Shanks, 1960; Wells, 1960). At the present time, three theories are generally accepted: one suggests a myogenic principle, another indicates some role of metabolic end-products, and a third invokes collapse of interlobular and arcuate veins. Proponents of each of these theories cite various lines of experimental evidence to support their theories which, at first glance, are mutually contradictory.

Evidence supporting a conclusion that the blood flow resistance change responsible for autoregulation is located in the interlobular and arcuate veins (Hinshaw, et al. 1959, 1961, 1963, 1964; Replogle, 1960a, 1960b, Wells, 1960) stimulated the study presented in this thesis. If resistance change concomitant with autoregulation is located in the renal veins, and is caused by a purely passive phenomenon of a transmural pressure difference causing collapse, the blood flow control mechanism must be non-linear. That is, fluid resistance at a given pressure in a section of collapsible vein is dependent upon blood

pressure upstream, and upon flow. Flow, in turn, depends on the resistance in the vein and resistance of the vasculature upstream. In such a control system it is difficult, if not impossible, to assess the effects of changes in the prevenous circulation on autoregulation in the venous circulation.

Equations are derived to describe the control of fluid flow through a simplified model of a section of the renal circulation. This mathematical model, when solved by a Runge-Kutta numerical technique, predicts (a) that autoregulation can occur by passive collapse of small renal veins, (b) that flow instability can arise as the result of a limit cycle, i.e. oscillation between two stable states. (The end of the collapsible tube where the transmural pressure is highest, the tube collapses to completely stop flow. Pressure immediately increases and tube reopens).

In order to observe the control mechanism postulated by the mathematical model in a real system, a hydraulic model was constructed using Tygon tubing to represent the non-collapsible arterial circulation and penrose surgical drainage tubing to represent the collapsible venous circulation. Autoregulation occurred in this model and its form was similar to that predicted by the mathematical model. Measurements were made of input pressure, output pressure, flow, and pressure within a water-filled chamber surrounding the penrose tubing through which water was flowing. The penrose tubing was analogous to a vein immersed in interstitial fluid. Several conclusions can be drawn from analyses of these data:

1. Autoregulation of fluid flow, similar to that seen in the kidney, can occur by the passive response of collapsible tubing to transmural pressure.

2. Because of the non-linear relationship between the area of the

collapsing tube and the transmural pressure, it is not necessary for chamber (interstitial) pressure to increase suddenly in order to produce autoregulation.

3. Oscillation in outlet pressure can be caused by a limit cycle when the resistance just upstream of the collapsible tube is low and the flow rate is high.

Measurement of blood flow rate, arterial pressure, and interlobular venous pressure (by retrograde insertion of a small cannula) were made on eight dog kidneys. Results indicate that the resistance change responsible for autoregulation takes place in the interlobular veins and the form of the pressure-flow curves approximates the form predicted by the mathematical model. The hypothesis of non-linear venous control of renal blood flow is compatible with other findings such as the concomitant release of metabolic end-products (Scott, 1965) because venous control is very responsive to changes elsewhere in therenal circulation.

References

1. Forster, R.P. and Maes, J.P. "Effect of Experimental Neurogenic Hypertension on Renal Blood Flow and Glomerular Filtration Rates in Intact Devervated Kidneys of Unanesthetized Rabbits with Adrenal Glands Demedullated," Amer. J. Physiol. 150:534, 1947.

2. Haddy, F.J. and Scott, J.B. "Role of Transmural Pressure in Local Regulation of Blood Flow through the Kidney," Am. J. Physiol. 208:825-831, 1965.

3. Hartmann, H. Orskov, S.L. and Rein, H. "Die Gefassreaktionen der Niere in Verlaufe Allgemeiner Kreislauf Regulatimsvorgange," Pflueger Arch. Ges. Physiol. 238:239, 1936.

4. Harvey, R.B. "Effects of Adenosine Triphosphate on Autoregulation of Renal Blood Flow and Glomerular Filtration Rate," Circu-

lation Research, Suppl. I to Vols 14 and 15:1-178 - 1-182, 1964.

5. Hinshaw, L.B. Day, S.B. and Carlson, C.H. "Tissue Pressure as a Causal Factor in the Autoregulation of Blood Flow in the Isolated Perfused Kidney," Amer. J. Physiol. 197:309, 1959.

6. Hinshaw, L.B. and Worthen, D.M. "Role of Intrarenal Venous Pressure in the Regulation of Renal Vascular Resistance," Circ. Res. 9:1156-1163, 1961.

7. Hinshaw, L.B. Brake, C.M. Iampietro, P.F. and Emerson, T.E. "Effect of Increased Venous Pressure on Renal Hemodynamics," Am. J. Physiol. 204(1):119-123, 1963.

8. Hinshaw, L.B. "Mechanism of Renal Autoregulation: Role of Tissue Pressure and Description of a Multifactor Hypothesis," Circ. Res. 14,15: Suppl. I, 120-131, 1964.

9. Replogle, C.R. Wells, C.H. and Collings, W.D. "Pressure-flow-distension Relationships in the Dog Kidney, Fed. Proc. 19: 360, 1960a.

10. Replogle, C.R. "Pressure-flow-distension Relationships in the Dog Kidney, Master's Thesis, M.S.U., 1960b.

11. Schmid, H.E. and Spencer, M.P. "Characteristics of Pressure-Flow Regulation by the Kidney," J. Appl. Physiology 17:201-204, 1962.

12. Scott, J.B. Daughtery, R.M. Dabney, J.M. and Haddy, F.J. "Role of Chemical Factors in Regulation of Flow through Kidney, Hind Limb, and Heart," Am. J. Physiol. 208:813-824, 1965.

13. Selkurt, E.E. "Relationship of Renal Blood Flow to Effective Arterial Pressure in the Intact Kidney of the Dog," Amer. J. Physiol. 147:537, 1946.

14. Waugh, W.H. and Shanks, R.G. "Cause of Genuine Autoregulation of the Renal Circulation," Circ. Res. 8:871-888, 1960.

15. Wells, C.H. "Estimation of Venous Resistance and their Significance to Autoregulation in Dog Kidneys," Master's Thesis, M.S.U., 1960.

A PROPOSED MODEL FOR RENAL BLOOD FLOW CONTROL

By

Clyde R. Replogle

A THESIS

Submitted to
Michigan State University
in partial fulfillment of the requirements
for the degree of

DOCTOR OF PHILOSOPHY

Department of Physiology

1967

Table of Contents

List of Illustrations

List of Tables

List of Appendices

A PROPOSED MODEL FOR RENAL BLOOD FLOW CONTROL

I. Introduction

The phenomenon of blood flow control intrinsic to an organ or segment of the circulation, without external control centers, is generally termed autoregulation. Autoregulation has been described in the liver (Torrance, 1958), skeletal muscle (Folkow, 1949), myocardium (Berne, 1959), brain (Rapela and Green, 1964), intestine (Johnson, 1960), and kidney (Selkurt, 1946). It has been found in humans, dogs, cats, rats, and calves. The form of pressure-flow curves can be quite different in each of these organs, and, because of the differences in blood flow rate per gram of tissue, interstital pressure levels, and reactivity to vasodilator metabolites, it is unreasonable to assume that autoregulation in the kidney and in other organs might have a common mechanism. Therefore, the model suggested in this thesis is proposed only for the kidney and autoregulation in other organs will be considered nowhere else in the thesis.

The first experiments on renal autoregulation were performed by Rein (1931) and later by Unna (1935), Hartmann (1936), and Forster and Maes (1947). These investigators concluded that an increase in systemic blood pressure causes an increase in resistance to blood flow resulting in less-than-proportional increase in renal blood flow, and that this phenomenon does not depend on neural connection to the rest of the body. Selkurt (1946) further characterized renal autoregulation as a means of control which only exists after arterial pressure exceeds 80 mm Hg. Below this

pressure, blood flow is directly proportional to pressure drop across the kidney. Since these first descriptions of renal autoregulation, many investigators have presented experimental evidence to support various opinions concerning the mechanism by which it occurs. The hypothesized mechanisms which are still widely accepted today may be divided into two types: active, (i.e., requiring energy expenditure by an effector), and passive (i.e., reacting to forces present within the circulation.

Three types of active control have been suggested: reaction to vasodilator metabolites, myogenic reaction to changes in transmural pressure, and a local reflex causing arteriolar vasomotion in response to pressure or flow within the kidney. All three of these types are active feedback control mechanisms. While the three mechanisms imply different sensing mechanisms to regulate flow, (response of general or specialized cells to decreased flow in the case of the metabolic mechanism, a flow or pressure sensor in the case of a local reflex mechanism, and inherent response to muscular arterioles in the case of the myogenic theory), and different control pathways (a chemical substance for metabolic control, neural pathways for a local reflex, and internal smooth muscle reaction for myogenic control), they all require a common effector, namely, the smooth muscle of the arteriole wall.

There is a good deal of evidence to suggest that a vasodilator metabolite is somehow connected to renal autoregulation. In early experiments, Winton (1934, 1951) and Bickford and Winton (1937) cooled dog kidneys in an isolated perfusion arrangement and found a decreased regulation with a concomitant increase in intrarenal pressure. This response

to temperature could easily be construed as affecting a metabolically dependent mechanism.

Haddy and co-workers (1958a) hypothesized that renal autoregulation was dependent on a metabolite, and that autoregulation of renal blood flow is dependent on blood flow rather than blood pressure. They based this conclusion on their findings that the onset of autoregulation appears at the same flow rate but at widely different arterial pressures, that lymph flow increases very little with increased arterial pressure, and that decapsulation does not decrease autoregulation.

Harvey (1964) showed that renal blood flow and glomerular filtration rate (GFR) (estimated by the product of directly measured renal plasma flow and creatinine extraction) were held relatively constant in spite of large changes in perfusion pressure in the isolated dog kidney. He further showed that adenosinetriphosphate (ATP) when infused into the renal artery could produce these results. He concluded that ATP produced dilation of the efferent arteriole. His work shows that a vasodilator metabolite could be released as a result of a decreased flow or pressure. Scott et al. (1965) substantiated this hypothesis by using the forelimb as an assay organ. They found that a vasodilator substance is released from the kidney when perfusion pressure was decreased. Scott and his co-workers found that adenosine, adenosine monophosphate (AMP), and ATP cause dilation in the forelimb but only ATP dilates the kidney. Also, they found that when ATP is infused into a kidney with the contralateral kidney as the assay organ, the target kidney shows dilation while the assay kidney shows constriction. As AMP has been found in re-

nal venous blood after reduction in perfusion pressure (Gordon, 1962), Scott and his co-workers interpreted their finding to mean that ATP is released when perfusion pressure is decreased. It then causes vasodilation and is then quickly converted to AMP or adenosine.

Winton (1964) attempted to show that autoregulation is "activated" by changes in velocity of blood flow rather than pressure differences across blood vessel walls. He obtained pressure-flow curves from control, epinephrine treated (0.4 to 14 mm^3 of 10 to 20 $\mu g\ ml^{-1}$ added as an impulse to each 0.6 ml of blood perfusing the kidney), and kidney cooled to 6-8° C. He then plotted resistance versus flow and resistance versus pressure. His curves show a better functional relationship between resistance and flow than for resistance and pressure. He cites this as evidence to support "a fairly clear indication of a flow - dependent mechanism". Even if his curves did support this conclusion, his method of calculating resistance produces a function which is unrelated to usual concepts of fluid resistance. He calculated resistance as the slope of the line connecting two adjacent points on a pressure-flow diagram, referred to the pressure mid-way between the two relevant pressures, divided by the slope of the line joining the origin to the point representing blood flow at 100 mm Hg. This calculation yields a normalized value of dP/dQ which has no physical significance. For example, if one has a system in which flow is constant for all values of pressure, Winton's method would calculate an infinite resistance for all

values of pressure and flow.

Bayliss (1902) and Folkow (1949) have shown that arteries and arterioles respond to an increase in intraluminal pressure by increasing the tone of their walls thereby decreasing their cross-sectional area and increasing their resistance. Waugh (1958, 1960) proposed that this myogenic, vasotonic reaction occurring in the afferent arteriole is the mechanism responsible for renal autoregulation. He based his conclusions on his findings that autoregulation is abolished by cyanide (suggesting an active process), that autoregulation is present after denervation (discounting a neural mechanism), and that there is a short delay of 2-3 seconds between the arterial pressure change and the onset of regulation. Semple and De Wardener (1959) measured arterial and venous pressure and flow in kidneys. By varying venous pressure they found that autoregulation depends on arteriovenous pressure difference rather than on the absolute pressure. They took this to indicate that the mechanism must involve the distension of small renal arteries and arterioles which causes a muscular reflex.

Haddy and Scott (1965) investigated the relationship between blood flow, arterial pressure, venous pressure, and pressure in an occluded hilar lymphatic vessel and found that hilar lymphatic pressure rises greatly on elevation of venous pressure but is little affected by a change in arterial pressure. They cite these data as evidence that the change in resistance caused by an increase in arterial pressure occurs in the arterioles. In the same study, Haddy and Scott were able to show that renal arterial pressure increases transiently for 2-4 seconds in response to a transient flow pulse lasting 0.5-2 seconds which they

state could represent a constriction (arteriolar) elicited by the stretch. They conclude that a myogenic response to a change in transmural pressure might assist the metabolic mechanism they have postulated (Scott, et al. 1965).

It is now interesting to note that while Haddy and co-workers (the strong proponents of a metabolic mechanism) have begun to suspect that there may be some myogenic responses creeping into their theory, Waugh (1964) (the strong proponent of a myogenic mechanism) has "tentatively suggested" that, while he is not going to throw out the transmural pressure idea altogether, autoregulation (still located in the afferent arterioles) may be dependent on variable metabolic feedback. This metabolic factor in turn is dependent on tubular re-absorption of glomerular filtrate and all are related finally to changes in transmural glomerular capillary pressure. His conclusions are based on some rather extensive observations on the fully isolated kidney. Measurement of intrarenal venous pressure (arcuate, interlobular) allowing division of renal resistance into prevenous and postvenous resistance indicate that the autoregulating resistance change is prevenous. Perfusion with a cell-free solution (e.g., 20% plasma - 80% PVP-Locke) resulted in good autoregulation thus eliminating a hematocrit change as important. A step increase in arterial pressure resulted in a transient, almost critically damped, pulse in flow with about a five second time constant, and a new, less-than-proportional, increase in steady state flow.

Waugh reports the observation of a "hunting-type" reaction of flow in response to a pressure step. But his curves show nothing more than a decrease in damping (approximately 3 cycles to half-amplitude rather

than approximately 0.8 cycles to half-amplitude, for his "non-hunting" kidney). The resistance of the higher damped kidney was 1.10 PRU before pressure step and 1.85 after, while the resistance of the underdamped kidney (treated with yohimbine to accomplish intrarenal sympatholysis) was 0.78 before pressure step and 1.28 after. The difference in his two responses could more easily be accounted for by the lower inertance and resistance of his treated kidney, rather than by a complex servomechanism "hunting" of a predetermined operating level. Waugh further observed that the flow response to a pressure step in a kidney in which the vascular reactivity was completely abolished by treatment with chloral hydrate, was also a step which changed proportionally more than pressure. This indicated to Waugh a mechanism which relies on vasomotion. By comparing the autoregulation capability of the same kidney one hour after isolation and three hours later (after mannitol diuresis) he was able to show that even though resistance had increased 4-5 times and flow reduced greatly, autoregulation responses were still good. He concluded that autoregulation is pressure dependent not flow dependent. Since glomerular filtration rate (GFR) is also autoregulated (Harvey, 1964; Schmid et al.,1964), Waugh contends that his observations confirm the concept of a preglomerular vasomotion change during regulation.

Waugh's final paragraph (Waugh, 1964) is as follows:

> "The reported experimental findings appear to support the hypothesis that myogenic vasomotor changes in the renal arterioles, in response to transmural arteriolar pressure, underlie active renal circulatory autoregulation. However, the experimental findings also support, perhaps more strongly, a new hypothesis that active renal circulatory autoregulation is accomplished by afferent arteriolar changes in resistance caused by tubular re-absorptive metabolism in response to flow of glomerular filtrate or to the level of glomerular transcapillary pressure."

Meanwhile, Schmid, who with Spencer in 1962 postulated an active feedback control system, has now (Schmid, et al, 1964) supported Waugh's old theory. Their first postulate was based on their observation that the renal pressure-flow curves are sharply inflected which, they maintained (without presenting evidence or logical argument), would exclude a passive mechanism. In their later experiments, Schmid and his coworkers found that blood flow is controlled by either a reduction in arterial pressure or increase in venous pressure and that GFR is also regulated in a like manner. They concluded that the regulation results from reduced pressure gradient and the resultant fall in transmural pressure of the preglomerular vessels.

In contrast to the active type of control demanded by the previous mechanisms, a passive feed-forward control has been postulated by Hinshaw (1959, 1960a, 1960b, 1960c, 1961, 1963a, 1963b, 1964), Replogle (1960a, 1960b), and Wells (1960). This mechanism is based on partial collapse of small intrarenal veins (interlobular) caused by a positive interstitial - intraluminal pressure difference. It is a passive control because no energy expending actuator is postulated and it is feed-forward control because the controlling variable (interstitial pressure) is derived upstream from the controlled variable (interlobular vein area).

The first evidence supporting this "tissue pressure" hypothesis came from two experiments (Hinshaw, 1960a; Replogle, 1960a, 1960b; Wells, 1960) using different indirect techniques to separate prevenous from postvenous resistance. These experiments show the autoregulating resistance changes occurring downstream from the glomerular capillaries (Hinshaw 1960a) and downstream from the peritubular capillaries (Replogle

1960a, 1960b; Wells, 1960). More recently Hinshaw (1960) and Section IV of this thesis show the resistance changes are located in the interlobular or arcuate veins.

Hinshaw (1959) blocked ureteral flow and, when ureteral pressure reached equilibrium, took the value of ureteral pressure as the pressure within Bowman's capsule. Having determined this pressure value, it is possible to calculate the pressure drop between the renal artery and Bowman's capsule (glomerular capillaries), and the pressure drop between the glomerular capillaries and the renal vein.

By plotting each of these pressure differences against flow, the amount of autoregulation in each section can be compared. Although the regulation in each segment is calculated in the same way, the manner in which an intrarenal pressure is obtained is different for each of the methods. Direct pressure values are obtained from a cannula inserted into an interlobular vein just short of the wedging point. The indirect method used by Replogle and Wells is more complicated. With the isolated kidney weighed continuously and flow blocked at the renal artery, renal venous pressure is increased in stages and a relationship between distending pressure and distension volume noted. With flow at zero, pressure throughout the kidney is the same and the distending pressure is taken to be the average pressure at the site of interstitial fluid formation. Flow through the kidney is then resumed and by measuring arterial pressure, flow rate, venous pressure, and kidney weight, the resistance of the segments of the circulation upstream and downstream from the transudation site can be calculated.

The disagreement between the direct small vein measurements of

Waugh (1964) and those of Hinshaw and Replogle, and the criticism of both techniques by Haddy and Scott (1965) are virtually the only controversies over data (see page 53 for discussion of Haddy's criticism and page 68 for discussion of Waugh's measurement). However, the controversy over possible mechanism is widening.

Perhaps the difficulties encountered in the attempt to merge the existing postulates and supporting data into a simple, and possibly correct, hypothesis are that the "criteria" (See Johnson, 1964) that have been suggested to separate the various mechanisms, and the "reasoning" used to reach the conclusions, have been largely intuitive.

By intuitive it is not meant that the proposed mechanisms and "critical experiments" were created from whole cloth, but that they have not been examined in the light of a rigorous description of renal fluid mechanics. Koch (1964) presented certain physical relationships which would exist in each of the proposed mechanisms by examining solutions obtained from idealized models. His approach, designed to provide a physical basis for separating one hypothesis from another, is certainly correct as far as he went. He did not, however, go beyond this to an illustrative solution of an entire control system.

The model proposed in this thesis is based on passive collapse of the interlobular veins. The study was stimulated by earlier work suggesting that the autoregulatory resistance changes take place in these veins, and by the desire to show how arteriolar changes would affect venous regulation. Some of the confusion surrounding explana-

tions for autoregulation can be explained by the non-linear relationships which must exist in such a passive control system. The collapsing pressure at any point in the veins is the difference between the extraluminal and intraluminal pressure at that point. The intraluminal pressure is a function of a) the resistance upstream from that point, b) the arterial pressure, and c) the flow. When the vessel collapses, its resistance increases, thereby changing the flow, and changing the variables on which collapsing pressure depends. It is very difficult to assess the influence of all of the fluid flow parameters in such a system by intuition alone.

It is the purpose of this study to describe mathematically a system which could operate to control renal blood flow in the venous circulation by passive means. A model is described which predicts the effects of the remainder of the renal circulation. Analysis of a hydraulic test model is presented to verify the mathematical model. Measurements of prevenous and postvenous regulation in the dog kidney are presented to verify the site of resistance change. Pressure-flow curves obtained from dog kidneys are compared with curves obtained from the hydraulic test model and predictions from mathematical theory. Results obtained by other investigators are examined in the light of the model.

II. Mathematical Model

Concept

The purpose of a model is to reduce a complicated system by imposition of assumptions and constraints to a simple system for which descriptions can be found and from which productive predictions of behavior of the complicated system can be made. If the modeling procedure has been correct, the mathematical description of the model is also the description of those aspects of the system that have been modeled.

The model presented here is restricted to operate on a principle compatible with operation in the renal venous circulation. That is, it must employ no mechanism that would depend upon active vasoconstriction. The mechanism is based on renal interstitial pressure arising by fluid leakage from the peritubular capillaries and renal tubules. An increase in interstitial pressure compresses the thin-walled veins. Although the model is concerned with a principle mechanism of change in resistance responsible for autoregulation located in the collapsible vessels, the resistances of the other segments of the renal circulation are considered as parameters affecting the control.

A simplifying assumption is made in considering the converging and diverging vessels of various diameters and wall thickness as single tubes. This assumption does not compromise the model, because the goal of the model is to show a principle on which renal autoregulation could operate, and not to predict the actual magnitude of the blood pressure at a specific location in a vein. The model is so con-

structed that it is consistent with renal anatomy in the sense that the same functional relationships between variables, such as pressure and flow, exist in the kidney as they do in the model.

It is also assumed that distributed points in the renal circulation can be modeled by discrete points. The error inherent in this assumption is dependent on the distance between the points. (See Appendix B for error analysis.) It is further assumed that the flow throughout the system is laminar. This has been shown to be the case by McDonald (1960).

Symbols used in the development of the model are shown in Table 1. In addition to definition of physical units, a functional notation (see Fig. 1) is shown in Table 2. The functional notation is used to describe locations within the kidney or model, and is used as subscripts to variables. In the description of a segment of circulation, the notation describing this segment is taken from the first point of reference to the next point of reference. That is, for example, the average flow between the inlet (Ø) and the leak point (S) is $Q_{Ø}$; the drop in pressure $P_{Ø} - P_S = \Delta P_{Ø}$; the resistance of this section = $R_{Ø}$. The control circuit segment is denoted by subscript c.

Derivation of Dynamic Equations of Motion for Model

Figure 2 shows a linear tube which is called "linear" because the area does not change as a function of any system variable, but the area can be made to change as a function of other inputs not considered.

Table I

Symbols

Symbol	Name	Units
A	area	cm^2
a	minor axis of ellipse	cm
b	major axis of ellipse	cm
c	circumference	cm
e	base of natural log	2.718 approximate
g	acceleration due to gravity	980.6 Dyne $cm^{-2}/cm\ H_2O$
L	fluid inertance	$cmH_2O\ sec^2\ cm^{-3}$ defined so that $\Delta P = L \frac{dQ}{dt}$ across an element
ℓ	length of tubing	cm
P	pressure	$cm\ H_2O$
Q	volume flow rate	$cm^3\ sec^{-1}$
R	resistance to fluid flow	$cm\ H_2O\ cm^{-3}$ sec; P = RQ
r	resistance per unit length	$cm\ H_2O\ cm^{-4}$ sec; $R = r\ell$
γ	shear stress	dyne cm^{-2}
μ	viscosity	dyne sec cm^{-2}
v	fluid flow velocity	cm sec^{-1}
x	variable distance	cm
ρ	fluid density	gm cm^{-3}
t	time	sec
ω	frequency	radians sec^{-1}

Table II Functional Notation and Systems Analogs

	Kidney		Model
Point a.	Point of hydraulic input to kidney - a point in the renal artery just outside the kidney	Point Ø.	hydraulic input to model
Point 1.	distributed point of exchange between circulation system and interstitial space. (glomerular capillaries to tubules to interstital space and peritubular capillaries to interstitial space).	Point S.	leak point
Point 2.	distributed point. Where the collapsability of the veins becomes large enough to allow them to change area with a pressure difference across the wall.	Point (2).	beginning of collapsible tube.
Point DV.	a point of measurement within the interlobular veins, upstream hydraulically from a point of maximum constriction.	Point CT.	a point within the collapsible tube which represents an average tube area.
Point V.	a point of measurement in the renal vein just outside the kidney.	Point 3.	a point at outlet of system.
Point I.	interstitial space	Point c.	any location within the pressure chamber surrounding the collapsible tube.

Figure 1 Control Model

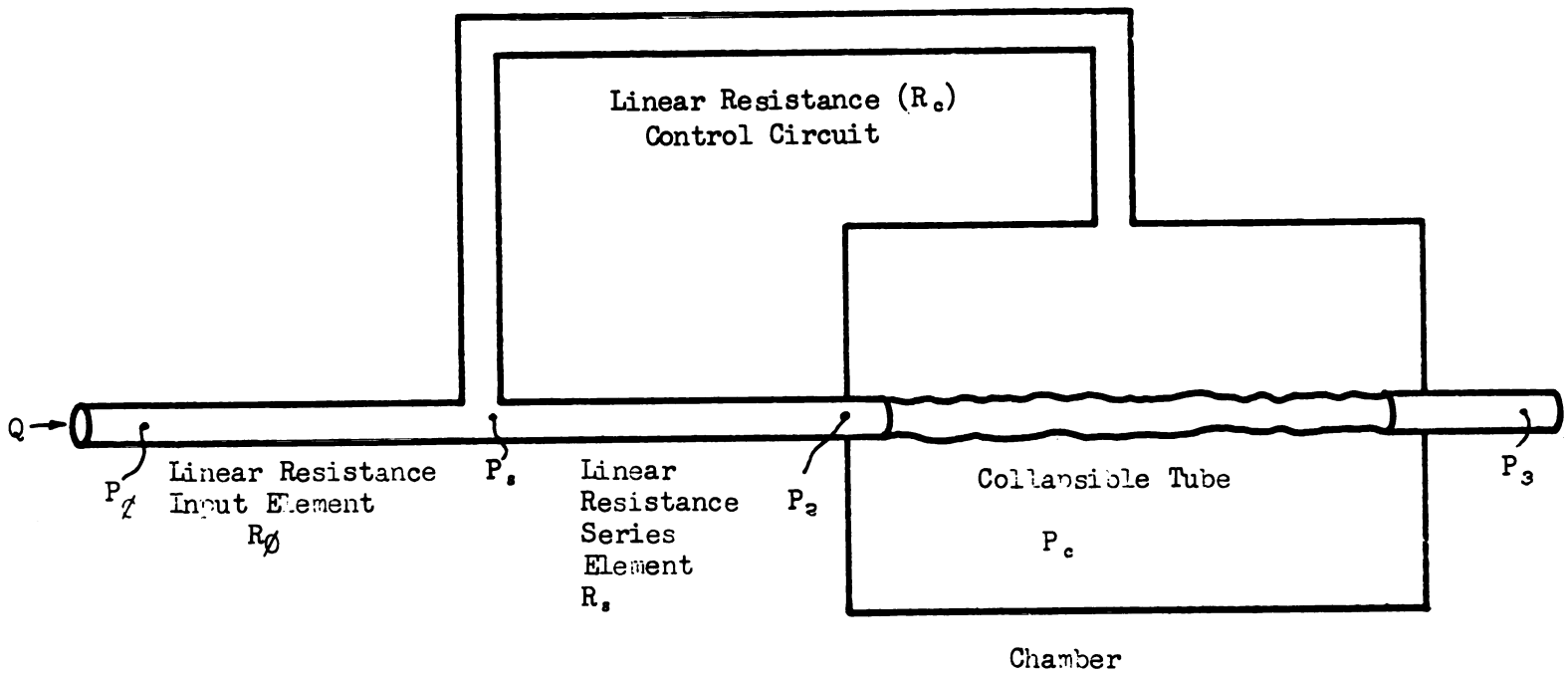

$P_\emptyset$ = Pressure at inlet to model

$R_\emptyset$ = Hydraulic resistance of linear section between inlet and leak point

$Q_\emptyset$ = Flow through section $\emptyset$

P_s = Pressure at leak point

Q_c = Flow in control circuit

R_c = Linear resistance of control circuit

P_2 = Pressure at beginning of collapsible tube

P_c = Pressure within chamber

P_3 = Pressure at outlet

Figure 2 Linear Resistance Tube

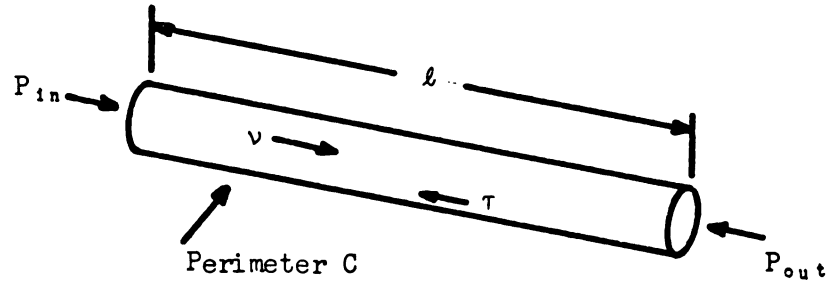

According to Newton's second law of motion, force equals mass times acceleration. Applying this principle to the fluid within a tube.

$$m \frac{dv}{dt} = g\ P_{in}\ A - g\ P_{out}\ A - c\tau\ell$$

Since the term "$c\tau\ell$" represents the frictional force, the term may be replaced by an equivalent force ($g\ R(\omega)\ Q\ A$) which is the pressure drop (due to friction) times the area. This yields:

$$m \frac{dv}{dt} = g\ P_{in}\ A - g\ P_{out}\ A - g\ R(\omega)\ Q\ A.$$

Further, $m = \rho A \ell$, and $v = \frac{Q}{A}$.

then, $\rho A \ell \frac{d}{dt} \left(\frac{Q}{A}\right) = g\ P_{in}\ A - g\ P_{out}\ A - g\ R(\omega)\ Q\ A.$

Canceling the area and expanding the derivative

$$\frac{d}{dt} \left(\frac{Q}{A}\right)$$

$$\frac{\rho \ell}{gA} \frac{dQ}{dt} = P_{in} - P_{out}\ R(\omega)Q.$$

Solving for P_{out}

$$P_{out} = P_{in} - R(\omega)\, Q - \frac{\rho \ell}{Ag} \frac{dQ}{dt}.$$

If $\frac{\rho \ell}{Ag}$ is defined as L (fluid inertance), and a correction factor (Stedman '56) is used to include the effect of frequency on the effective mass, the equation becomes:

$$P_{out} = P_{in} - R(\omega)\, Q - L(\omega) \frac{dQ}{dt}. \tag{1}$$

Applying this equation to each linear element (see Fig. 1) provides the required set of dynamic equations. These are:

$$P_s = P_\emptyset - R_\emptyset(\omega)\, Q_\emptyset - L_\emptyset(\omega) \frac{dQ_\emptyset}{dt} \tag{2}$$

$$P_2 = P_s - R_s(\omega)\, Q_s - L_s(\omega) \frac{dQ_s}{dt} \tag{3}$$

$$P_c = P_s - R_c(\omega) Q_c - L_c(\omega) \frac{dQ_c}{dt}. \tag{4}$$

In addition to the above, an equation of continuity may be written for the junction point (see Fig. 1):

$$Q_\emptyset = Q_s + Q_c. \tag{5}$$

This completes the derivation of the continuity and momentum equations for the linear elements. Although an energy equation could be derived, it is not independent and provides no new information.

The methods of Shapiro (1953), for compressible fluid dynamics, are used to derive the collapsible tube equations because a simple relationship exists between compressible flow in incompressible tubes and incompressible flow in compressible tubes. The equations are written for the fluid in a control volume (Fig. 3) defined by the walls of

the collapsible tube. It has been assumed that the tube collapses in an elliptical shape of constant circumference which holds for the values of pressure and flow where regulation occurs.

The principle of conservation of mass may be applied to the fluid in the control volume to derive the continuity equation. That is, the time rate of change of mass in the control volume is equal to the rate at which it enters one end minus the rate at which it leaves the other (see Fig. 3c). Or,

$$\frac{\partial}{\partial t}(\rho A dx) = \rho Av\Big|_x - \rho Av\Big|_{x+dx}$$

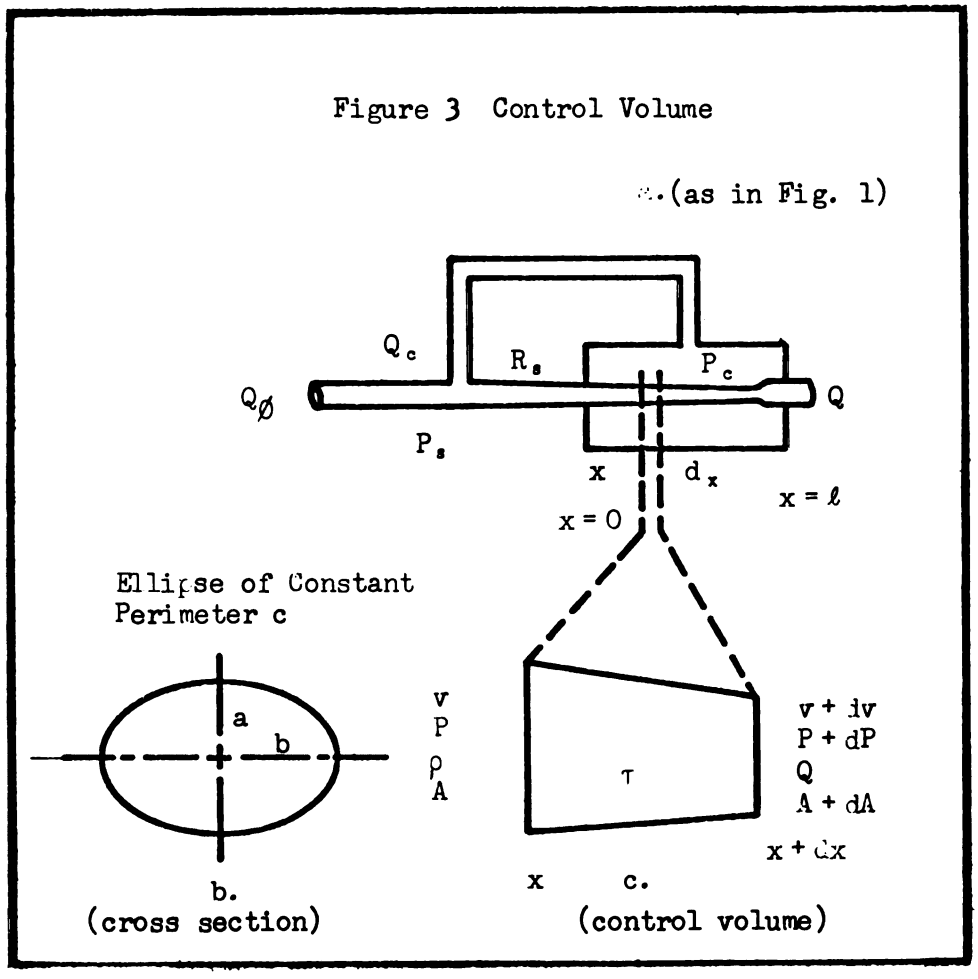

Figure 3 Control Volume

(as in Fig. 1)

Expanding ρAv in a Taylor series about x,

$$\rho Av\Big|_{x+dx} \approx \rho Av\Big|_{x} + \frac{\partial}{\partial x}(\rho Av)dx,$$

which will yield

$$\frac{\partial}{\partial t}(\rho A dx) = \frac{-\partial}{\partial x}(\rho Av)\, dx.$$

Since the fluid is incompressible and x is not a function of time,

$$\frac{\partial A}{\partial t} + \frac{\partial (Av)}{\partial x} = 0. \tag{6}$$

Newton's second law may be applied to yield the momentum equation. That is, the time rate of change of momentum in the control volume is equal to the net rate of momentum entrance plus the sum of the forces. Or,

$$\frac{\partial}{\partial t}(\rho Avdx) = \rho Av^2\Big|_{x} - \rho Av^2\Big|_{x+dx} + gPA\Big|_{x} - gPA\Big|_{x+dx} + g\left(P + \frac{dP}{2}\right)\frac{dA}{dx}dx - c\tau dx.$$

Again, expanding in a Taylor series,

$$\frac{\partial}{\partial t}(\rho Avdx) = \rho Av^2\Big|_{x} - \left[\rho Av^2\Big|_{x} + \frac{\partial}{\partial x}(\rho Av^2)\, dx\right] + gPA\Big|_{x} - g\left[PA\Big|_{x} + \frac{\partial}{\partial x}(PA)\, dx\right] + g\left(P + \frac{dP}{2}\right)\frac{dA}{dx}dx - c\tau dx.$$

or,

$$\frac{\partial}{\partial t}(\rho Avdx) = \frac{-\partial}{\partial x}(\rho Av^2)\, dx - g\frac{\partial (PA)}{dx}dx + gP\frac{\partial A}{dx}dx + gP\frac{dP}{2}\frac{\partial A}{\partial x}dx - c\tau\, dx.$$

If the higher order differentials are neglected, and the derivative of

PA expanded,

$$\frac{\partial}{\partial t}(\rho A v dx) = \frac{-\partial}{\partial x}(\rho A v^2)\, dx - g\, A \frac{dP}{dx} dx - c\tau\, dx.$$

This reduces to

$$\rho \frac{\partial (Av)}{\partial t} + \rho \frac{\partial}{\partial x}(Av^2) + g\, A \frac{\partial P}{\partial x} + c\tau = 0.$$

Expanding the differentials,

$$\rho A \frac{\partial v}{\partial t} + \rho v \cancel{\frac{\partial A}{\partial t}} + \rho v \cancel{\frac{\partial (Av)}{\partial x}} + \rho A v \frac{dv}{dx} + g\, A \frac{dP}{\partial x} + c\tau = 0$$

and subtracting ρv times the continuity equation (6) eliminates the terms indicated. The equation then becomes,

$$\rho A \frac{\partial v}{\partial t} + \rho A v \frac{\partial v}{\partial x} + g\, A \frac{\partial P}{\partial x} + c\tau = 0.$$

Since the term "$c\tau$" represents the forces per unit length due to friction, it may be replaced by an equivalent force of the pressure drop due to friction per unit length times the area. Therefore, since $c\tau = grQA$, where r is the resistance of the tube per unit length,

$$\rho A \frac{\partial v}{\partial t} + \rho A v \frac{\partial v}{\partial x} + g\, A \frac{\partial P}{\partial x} + grQA = 0.$$

It can be shown (see Appendix A) that for an elliptical tube of constant perimeter, $r = r' \frac{(A')^3}{A^3}$, where r' is the resistance per unit length of the tube when it is circular and has the area A'. The equation then becomes:

$$\rho A \frac{\partial v}{\partial t} + \rho A v \frac{\partial v}{\partial x} + g\, A \frac{\partial P}{\partial x} + gr' \frac{(A')^3}{A^2} Q = 0. \qquad (7)$$

The volume flow rate can be expressed in terms of area and velocity:

$$Q = Av. \tag{8}$$

The three differential equations (2,3,4) for the linear elements are coupled to the two differential equations (6,7) for the fluid in the collapsible tube. One coupling relation is the mechanical properties of the collapsible tube which will be called the "equation of state" and which must be determined experimentally (see page 44). The relationship is: $A(x) = f(P_c - P(x))$. For $\frac{3}{8}$" diameter penrose tubing the function is:

$$A(x) = 0.362\, e^{-0.159(P_c - P(x))^2} + 0.105\, e^{-0.0061(P_c - P(x))^2} + \frac{0.0398}{(P_c - P(x) + 1)^{0.2}} + 0.03. \qquad \text{(see page 46)} \tag{9}$$

A second coupling relation can be deduced by relating the area of the collapsible tube to flow through the control circuit (c). Since the chamber containing the collapsible tube is rigid, the net volume of the chamber is a constant. Therefore, the flow equals the net rate at which the tube is contracting:

$$Q_c = \frac{-\partial}{\partial t} \int_o^{\ell} A dx. \tag{10}$$

For the real kidney and in a model used to test the effect of the stiffness of the renal capsule, the increase in volume of the system must be measured and equation (10) becomes:

$$Q_c = \frac{-\partial}{\partial t} \int_o^{\ell} A dx + \frac{dv}{dt},$$

where v is the volume of the chamber.

The third coupling relation is the overall energy rate equation

for the chamber containing the collapsible tube. For the purpose of this derivation, energy dissipated due to friction may be considered lost because it can never be converted back to mechanical energy within the system. Within the chamber as a control volume, the time rate of change of energy stored is equal to the net rate at which kinetic energy enters plus the net rate at which work is done on the system minus the rate at which energy is dissipated due to friction. Or,

$$\frac{\partial}{\partial t}\int_0^{\ell}\left(\frac{\rho A v^2}{2g} + \text{P.E.}\right) dx = \frac{\rho A_c v_c^3}{2g} + \frac{\rho A_s v_s^3}{2g} -$$

$$\frac{\rho A_3 v_3^3}{2g} + P_c Q_c + P_2 Q_s - P_3 Q_3 - r' \frac{(A')^3}{A^3} Q^2 \, dx \qquad (11)$$

where P.E. is the potential energy per unit length stored in the walls of the collapsible tube. The potential energy stored in the tube is equal to the work done on the tube in compressing it from the initial area A' to the final area. That is,

$$\text{P.E.} = \int_0^{P_c - P} (\text{pressure difference})\,(\text{change in volume})$$

$$= \int_0^{P_c - P} \alpha \cdot dA(\alpha) \cdot 1$$

or since

$$dA(\alpha) = \frac{\partial A(\alpha)}{\partial x} d\alpha,$$

$$\text{P.E.} = \int_0^{P_c - P} \alpha \frac{\partial A(\alpha)}{\partial \alpha} d\alpha = h\,(P_c - P).$$

Substituting

$$v_c = \frac{Q_c}{A_c},\ v_s = \frac{Q_s}{A_s},\ Q_s = Q_\emptyset,\ \text{and}$$

$v_3 = \frac{Q_\emptyset}{A_3}$, and setting $P_3 = 0$ reduce Eq. 11 to

$$\frac{\partial}{\partial t}\int_0^{\ell}\left[\frac{\rho A v^2}{2g} + h\,(P_c - P)\right]dx = \frac{\rho}{2gA_c^2}Q_c^3 + \frac{\rho}{2gA_s^2}Q_3^3 -$$

$$\frac{\rho}{2gA_3^3}Q_\emptyset + P_c\,Q_c + P_2\,Q_s - \int_0^{\ell} r'\,\frac{(A')^3}{A^3}Q^2\,dx.$$

In summary, the complete set of equations consist of:

$$P_1 = P_\emptyset - R_\emptyset\,Q_\emptyset - L_\emptyset\frac{\partial Q_\emptyset}{\partial t} \tag{2}$$

$$P_2 = P_1 - R_s\,Q_s - L_s\frac{\partial Q_s}{\partial t} \tag{3}$$

$$P_c - P_1 - R_c\,Q_c - L_c\frac{\partial Q_c}{\partial t} \tag{4}$$

$$Q_\emptyset = Q_s + Q_c \tag{5}$$

for the linear elements, and

$$\frac{\partial A}{\partial t} + \frac{\partial (Av)}{\partial x} = 0 \tag{6}$$

$$\rho A\frac{\partial v}{\partial t} + \rho Av\frac{\partial v}{\partial x} + g\,A\frac{\partial P}{\partial x} + gr'\frac{(A')^3}{A^2}Q = 0 \tag{7}$$

$$Q = Av \tag{8}$$

for the collapsible tube, and

$$A = f\,(P_c - P) \tag{9}$$

$$Q_c = \frac{-\partial}{\partial t}\int_o^{\ell} A dx$$

$$\frac{\partial}{\partial t}\int_o^{\ell}\left(\frac{\rho A v^2}{2g} + h\right) dx = \frac{\rho}{2g}\left(\frac{Q_c^3}{A_c^2}\frac{Q_c^3}{A_s^2}\frac{Q_\phi^3}{A_3^2}\right) +$$

$$+ P_c Q_c + P_2 Q_s - \int_o^{\ell} r'\frac{(A')^3}{A^3} Q^2 dx \qquad (12)$$

for the coupling relations. This set of ten equations in ten unknowns could (in principle) be solved to establish the dynamic behavior of the system.

Steady Flow Equations and Boundary Conditions

When the flow is not changing with time, the equations describing the system are reduced considerably. Under these conditions, the differential equations may be integrated numerically with a Runge-Kutta technique or by direct integration if the relationship between area and pressure in the collapsible tube is simple. The set of equations for steady flow reduces to:

$$P_c = P_1 \qquad (13)$$

$$P_2 = P_1 - R_s Q \qquad (14)$$

$$Q = Av \qquad (8)$$

$$\frac{d(Av)}{dx} = 0 \qquad (15)$$

$$\frac{\rho A v}{g}\frac{dv}{dx} + \frac{A dP}{dx} + r'\frac{(A')^3}{A^2} Q = 0 \qquad (16)$$

$$A = f(P_c - P) \qquad (9)$$

This set of equations may be modeled in the following manner. There is a relationship between P_2, P_c, and Q within the collapsible tube; $Q = g(P_2, P_c)$, which is represented below.

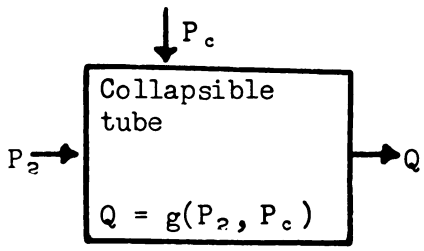

The linear element also has a transfer function $P_2 = P_1 - R_s Q$

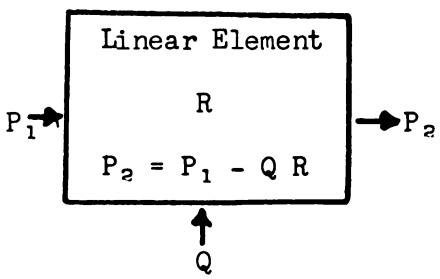

In the closed loop configuration these two elements are connected so that $P_c = P_s$ (see Fig. 4).

Figure 4. Closed Loop Configuration

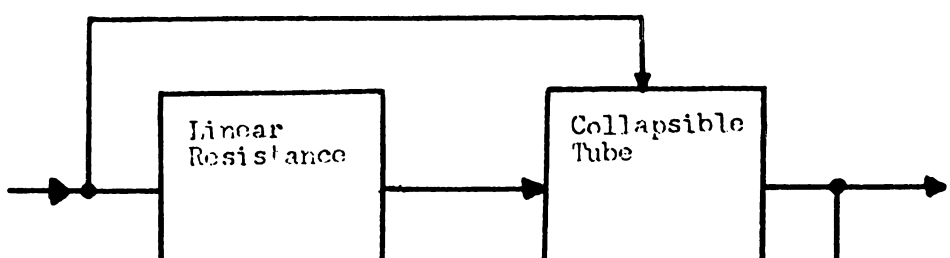

The method used to solve the system shown in Fig. 4 is to determine the transfer function $Q = g(P_2, P_c)$, and then close the loop $P_c = P_s$ to find the relation $Q\emptyset = Q(P_1)$. Fig. 4 shows that there are actually two control paths. The input pressure is "fed forward" (a) to apply pressure to the collapsible tube and the flow rate is "fed back" (b) to the linear resistance. To solve the set of equations (8,9,13,14,15,16), the differential equation for the collapsible tube must be put in a form suitable for the use of Runge-Kutta techniques. Expanding 15,

$$A \frac{dv}{dx} + v \frac{dA}{dx} = 0.$$

or,

$$\frac{dv}{dx} = - \frac{v}{A} \frac{dA}{dx} .$$

Putting this into (16) yields

$$- \frac{\rho v^2}{g} \frac{dA}{dx} + A \frac{dP}{dx} + \frac{r'(A')^3 Q}{A^2} = 0.$$

But from (8),

$$v = \frac{Q}{A}.$$

Hence,

$$- \frac{\rho Q^2}{gA^2} \frac{dA}{dx} + A \frac{dP}{dx} + \frac{r'(A')^3 Q}{A^2} = 0. \qquad (17)$$

If it is assumed that the area of the collapsible tube is a simple function of pressure (i.e., such as $A = P_c - P$) then,

$$\frac{dA}{dx} = \frac{dA}{dP} \frac{dP}{dx}.$$

Therefore,

$$-\frac{\rho Q^2}{gA^2}\frac{dA}{dP}\frac{dP}{dx} + A\frac{dP}{dx} + \frac{r'(A')^3 Q}{A^2} = 0.$$

Solving for $\frac{dP}{dx}$,

$$\frac{dP}{dx} = \frac{-r'(A')^3 Q}{A^3 - \frac{\rho Q^2}{g}\frac{dA}{dP}}. \tag{18}$$

This is in the required form for integration by a Runge-Kutta technique (i.e., $\frac{dP}{dx} = \gamma\ (P)$).

In the real kidney, however, the area of the collapsible veins would not be expected to be a simple function of pressure difference across the walls. Collapsibility of the veins varies from venule to renal vein as the diameter and wall thickness increases. The assumption of variable properties only slightly complicates the mathematical solution. A more general case would assume that radius and area are functions of distance along the collapsible tube. ($r' = r'(x)$; $A' = A'(x)$, $A = f(P_c, P_s, x)$. In this case

$$dA = \frac{\partial A}{\partial x}dx + \frac{\partial A}{\partial P}dP,$$

and

$$\frac{dA}{dx} = \frac{\partial A}{\partial x} + \frac{\partial A}{\partial P}\frac{dP}{dx}.$$

Putting this into equation (17) and multiplying by A^2,

$$-\frac{\rho Q^2}{g}\frac{\partial A}{\partial x} - \frac{\rho Q^2}{g}\frac{\partial A}{\partial P}\frac{dP}{dx} + A^3\frac{dP}{dx} + r'(x)^3 Q = 0$$

again solving for $\frac{dP}{dx}$, $\frac{dP}{dx} = \frac{\frac{\rho Q^2}{g}\frac{\partial A}{\partial x} - r'(x)\,A'(x)^3 Q}{A^3 - \frac{\rho Q^2}{g}\frac{\partial A}{\partial P}}$ (19)

Equation (19) is of the form.

$$\frac{dP}{dx} = \gamma\ (P,x),$$

and hence can be solved by a similar Runge-Kutta technique. Even though there may be some variations in tube properties with distance, a reasonable approximation for the present series of experiments is that the tube area is only a function of collapsing pressure (Eq. 18).

Figure 5

End Boundary Conditions of the Collapsible Tube

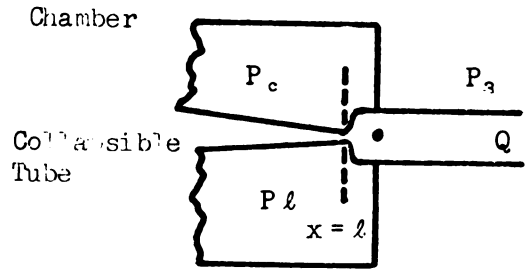

The boundary condition at $x = \ell$ is derived from Venard ('57),

$$P_\ell + \frac{v_\ell^2}{2g} = P_3 + \frac{v_3^2}{2g} + K\,\frac{(v_\ell - v_3)^2}{2g}$$

where K is a discharge coefficient, for a sharp area transition, K is usually taken to be one (1). Setting K = 1, and solving for P_ℓ,

$$P_\ell = \frac{v_3^2 - v_\ell\, v_3}{g}$$

or,

$$P_{\ell} = \frac{Q^2}{gA_3^2} - \frac{Q^2}{gA_3 A_{\ell}} \tag{20}$$

this is the required boundary condition at $x = \ell$

Summary

A set of equations is derived for a system which models blood flow regulation in the kidney. The system contains two control loops which can regulate rate of flow. These equations can be solved by an iterative, third-order Runge-Kutta technique to show the relationships between pressure input (P_2) and flow (Q) through the system with the series resistance (R_s) as a parameter.

Computer Solutions

A computer program was written for the IBM 7094 to solve equation (18) subject to the boundary conditions of equations (14) and (20). The logical sequence followed by the programs to solve for open loop response, closed loop response, and pressure distribution along the collapsible tube is shown in Appendix B.

The parametric fluid flow curves predicted by the computer program are shown in Fig. 6. Two results of this simulation seem significant. With the range of R_s used, the curves (when corrected with a dimensional analysis for the difference between blood viscosity and water viscosity, i.e., P multiplied by 4) fall into the pressure-flow range for the kidney and exhibit similar regulation characteristics. Also, the results predict a region of instability where the flow rate would oscillate. This unstable region has also been noted in the kid-

Figure 6 Computer Results for Closed Loop Operation

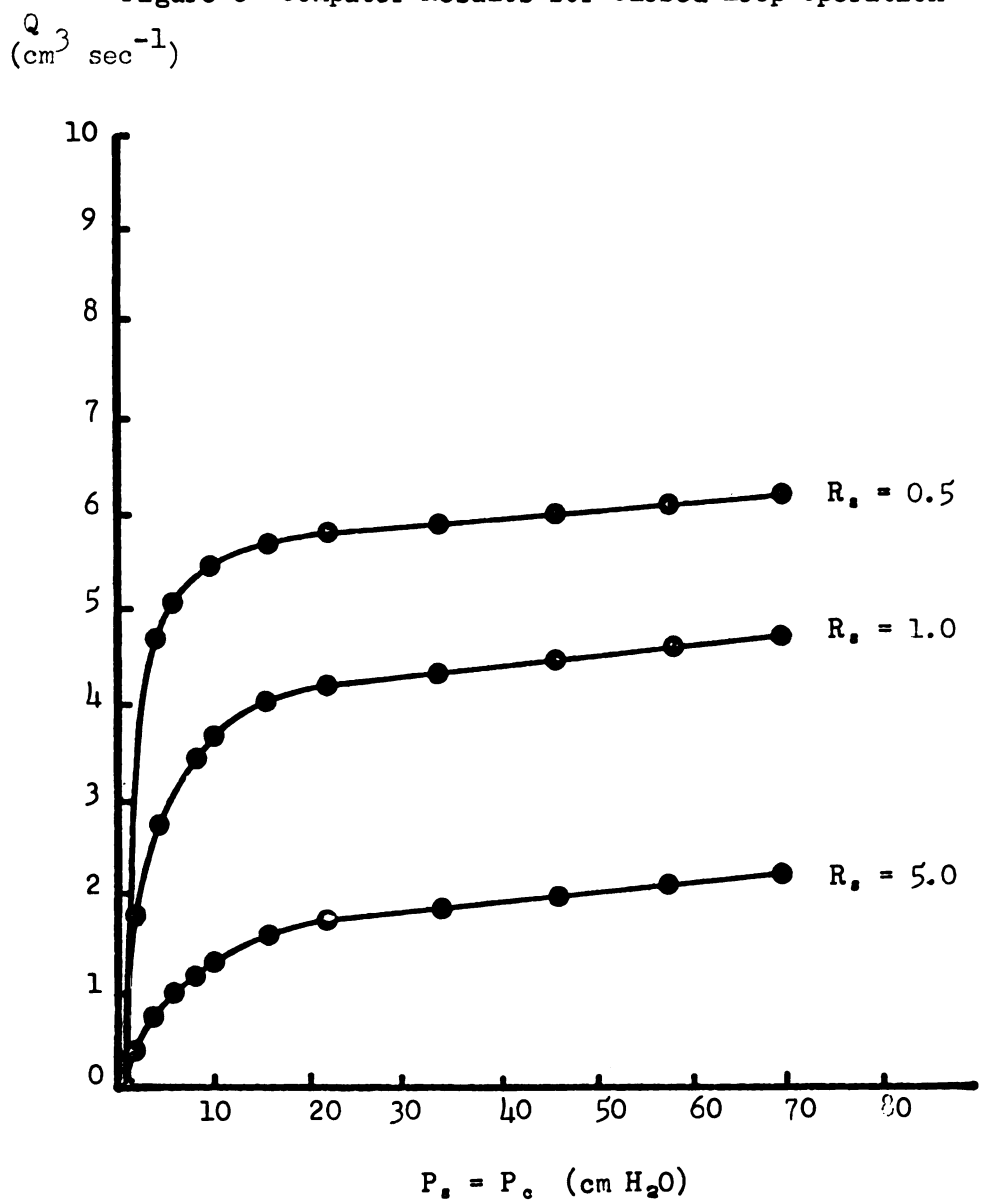

ney (Replogle, 1960; Hinshaw, 1961). An explanation of the instability can be found by examination of the denominator of equation (18).

$$\frac{dP}{dx} = - \frac{r'(A')^3 Q}{A^3 - \frac{{}^0Q^2}{g} \frac{dA}{dP}} \tag{18}$$

As Q increases there is a point where the denominator approaches zero for a given value of A and $\frac{dA}{dP}$. The mathematical interpretation is that as Q approaches a value which makes the denominator zero, the steady flow equation no longer describes the system. This means that the flow is no longer time independent but is oscillating. For any given difference in pressure (P_c - P), A and $\frac{dA}{dP}$ may be calculated from equation (9). Solving the equation (Denominator of Eq. 18),

$$A^3 = \frac{{}^0Q^2}{g} \frac{dA}{dP} = 0 \tag{21}$$

for Q, predicts the maximum flow rate (Q_{max}) for which steady flow equations apply. The solution is plotted in Fig. 7. This procedure, however, has a limitation in that it can predict the upper limit of steady flow but not the actual flow rate at which the system will oscillate.

The predicted open loop curves are plotted in Fig. 8 and the predicted pressure distribution along the collapsible tube are plotted in Figs. 9 and 10.

Figure 7 Prediction of Stability

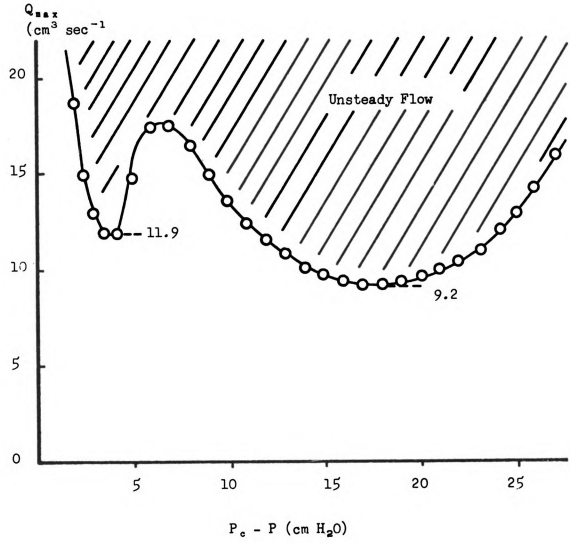

Figure-8 Computer Results for Open Loop Operation

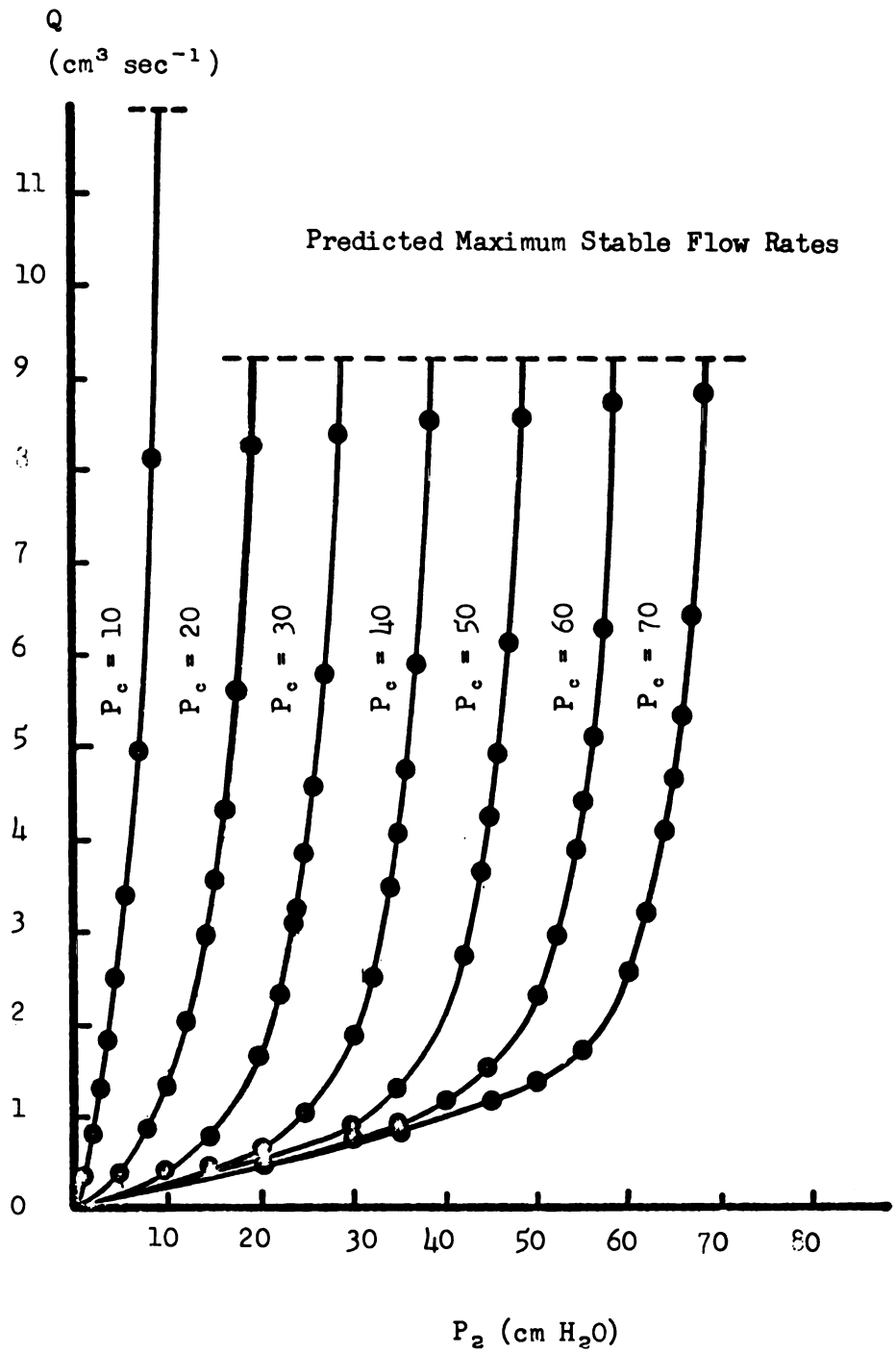

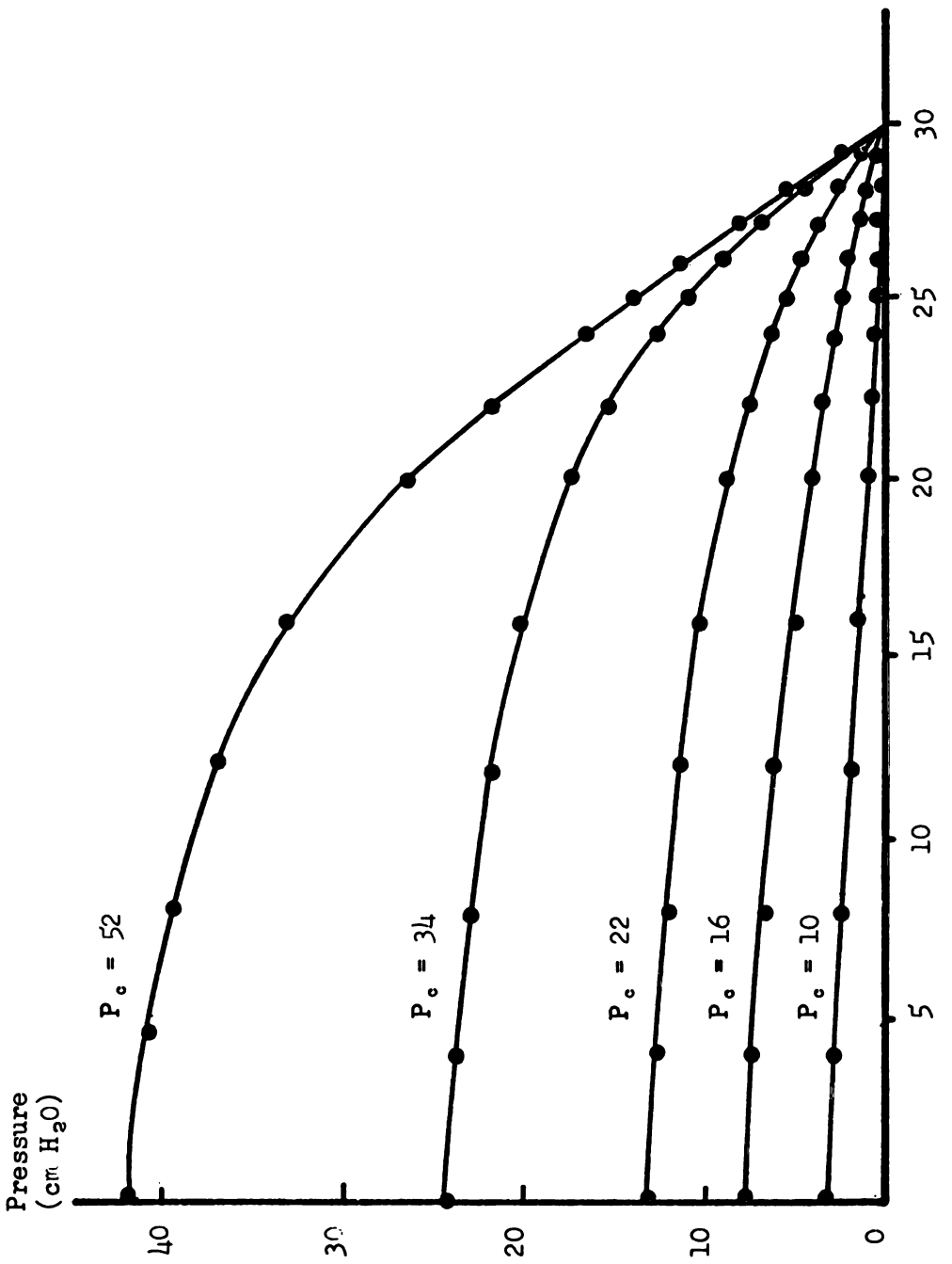

Figure 9 Pressure Distribution Along Collapsible Tube

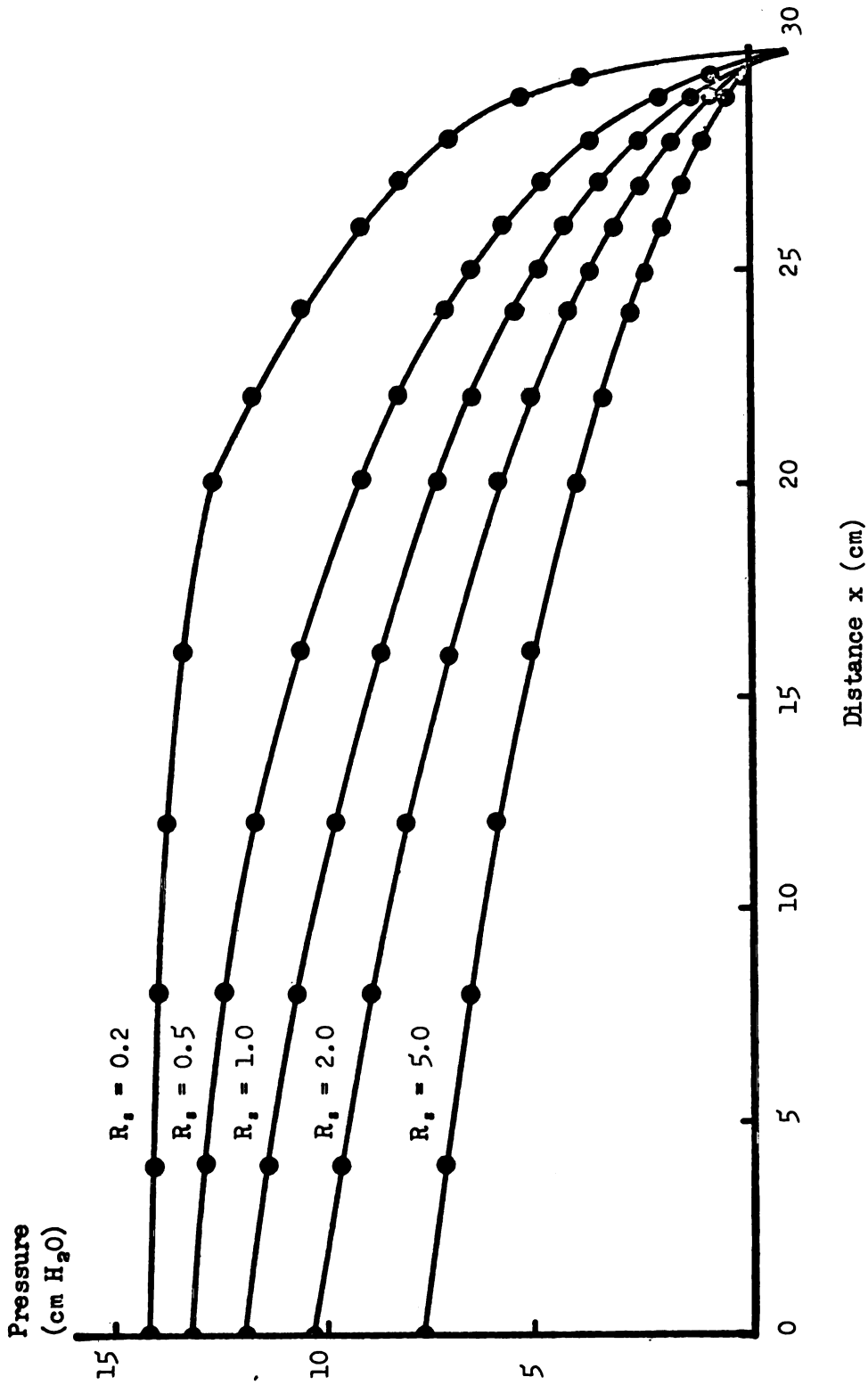

Figure 10 Pressure Distribution Along Collapsible Tube

III. Hydraulic Test Section

In order to check the predictions made by the computer analysis, a mechanical model was constructed. The use of a mechanical model to check predictions has several advantages. The mechanical model can be made to conform exactly with the assumptions made for the equations eliminating questions concerning initial hypothesis of mechanism. The model provides access to variables that are impossible to measure directly in the kidney. Most important perhaps, is that it provides a "proof of existence". That is, if a model can be made to control flow using the mechanism postulated to exist in the kidney, at least it could work this way in the kidney.

Pressure Supply

The pressure supply (Fig. 11) consists of a variable height overflow reservoir. Water enters at the top of a 6 inch diameter, 5 foot high metal cylinder. Two $\frac{3}{4}$ inch diameter tubes are welded to the bottom of the cylinder. One tube supplies constant pressure to the test section while the other is attached to a variable height reservoir. The overflow consists of two sections of $\frac{3}{4}$ in. I.D. flexible tubing connected to a pipe tee. The pipe tee is clamped to a circular rod so that the level of the overflow can be changed. A sight gauge is also provided so that the applied pressure can be read directly in cm H_2O. The system can hold pressure constant within $\pm$ 0.1 cm H_2O.

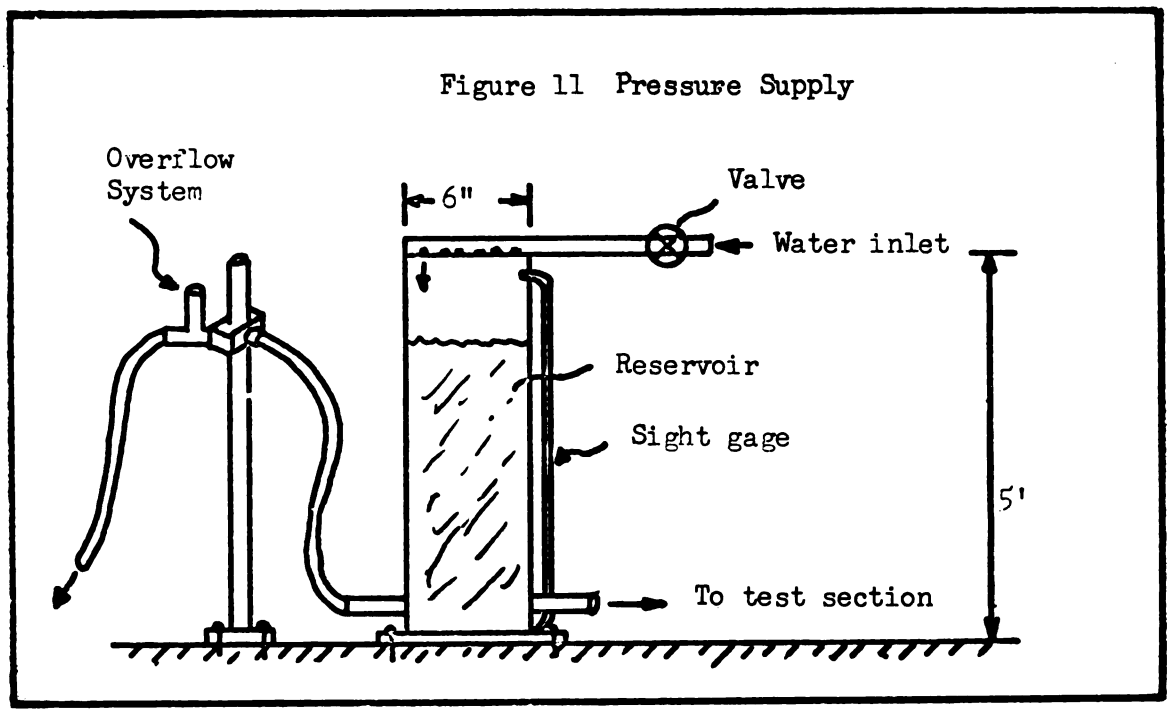

Figure 11 Pressure Supply

Test Section

Water from the supply flows into the test section (Fig. 12) through a ¾" I.D. Tygon tube which is fitted with an electromagnetic flow transducer (¾" I.D. Medicon, Model C59-f18). The test section consists of two Tygon tubes, three pressure fixtures, and a plastic chamber containing the collapsible tube.

The pressure fixture is shown in Fig. 13. It is constructed of a 6" long stainless steel tube of a diameter to match the collapsible tube. Four inches from the inlet (over 10 diameters) an 0.050" I.D. tube, 1½" long is silver soldered to the large tube. Flanges are provided for mounting.

Figure 12 Test Section

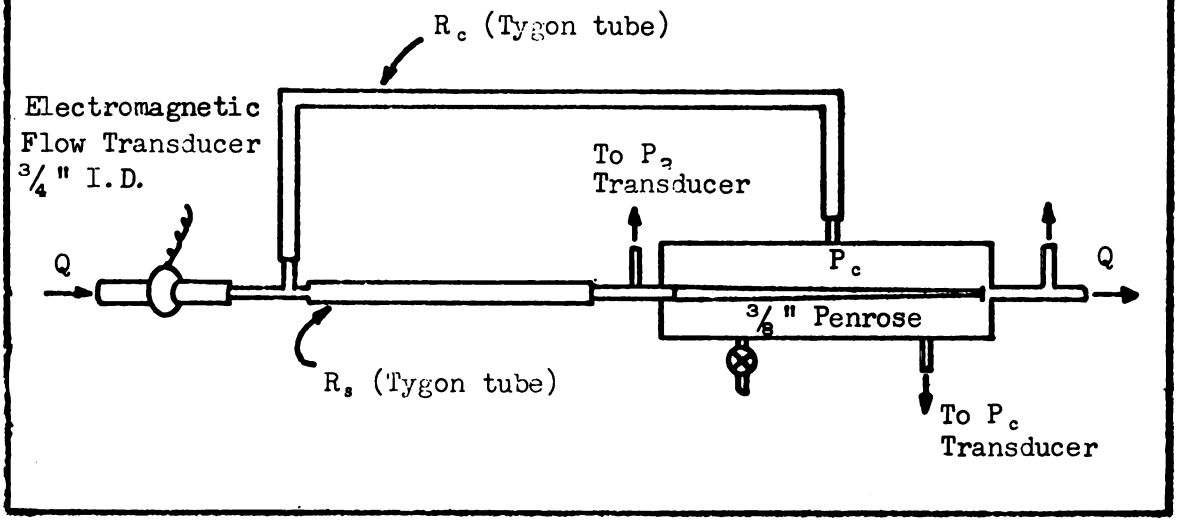

Figure 13 Pressure Fixture

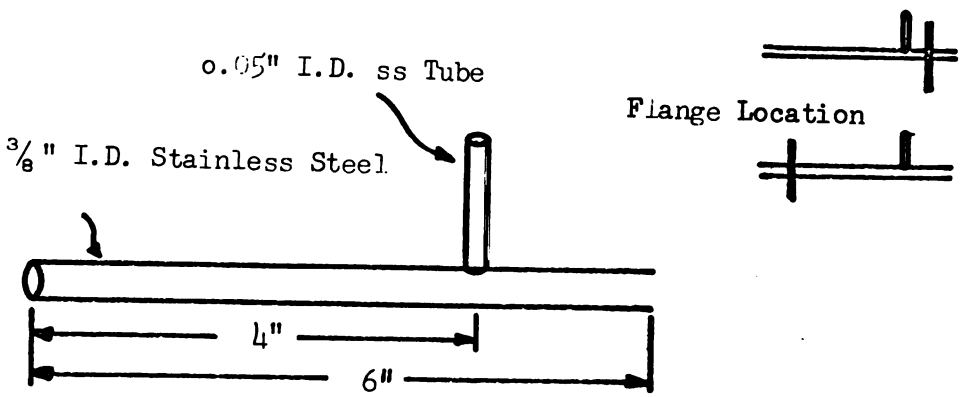

Figure 14 Chamber for Collapsible Tube

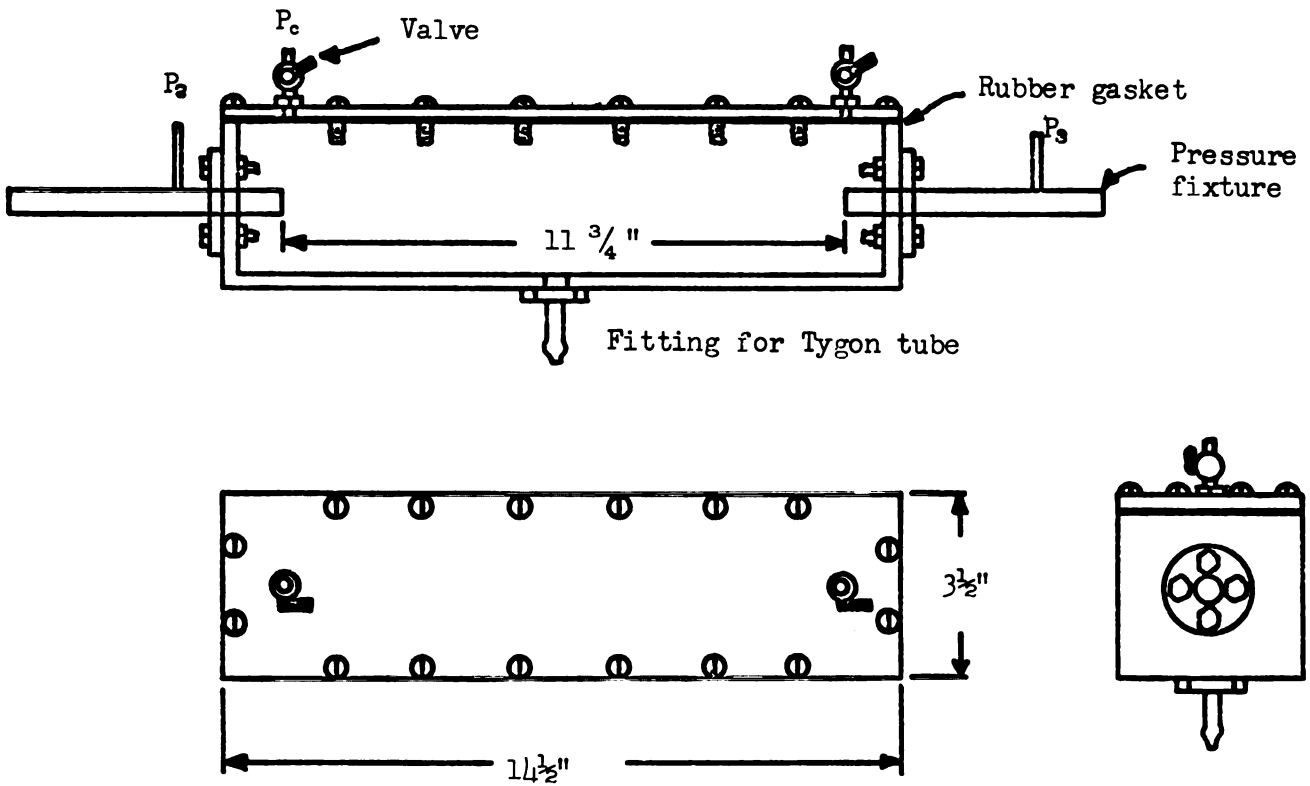

The chamber (Fig. 14) is constructed of clear plastic so that the collapsible tube can be observed. Two-way valves are cemented into the top for connection to pressure transducer, elastic reservoir, or independent pressure source.

Methods of Measurements

The instrumentation consists of three pressure transducers (Statham P23AA and P23Db) used to measure P_c, P_2, and P_3, and a large flow transducer (Medicon Model C59-F18) connected to an electromagnetic flow meter (Medicon Model Fm-6R). The signals from the three channels of pressure and flow channel were recorded on an Electronics for Medicine Model DR-8, Simultrace Recorder. Care was taken to assure the absence of bubbles in the water supply in order to avoid interference with the flowmeter. The frequency response of the system is entirely adequate to record the 3-4 Hz oscillation which characterized the instable regions of the tubing studied.

Three different measurements were taken in the system; (1) measurement of the area of the collapsible tube as a function of pressure (the "equation of state"), (2) measurement of the open loop characteristics of the system, and (3) measurement of closed loop characteristics. The area of the collapsible tube as a function of the pressure difference across the wall was measured using the system pictured in Fig. 15. A zero level is adjusted so that the system is full of water and the collapsible tube has a circular cross-section. The chamber is then pressurized by pouring water in the top of the manometer. For each level above the zero point, the amount of fluid which has left the

Figure 15

Configuration for Measurements of
Area as a Function of Collapsing Pressure

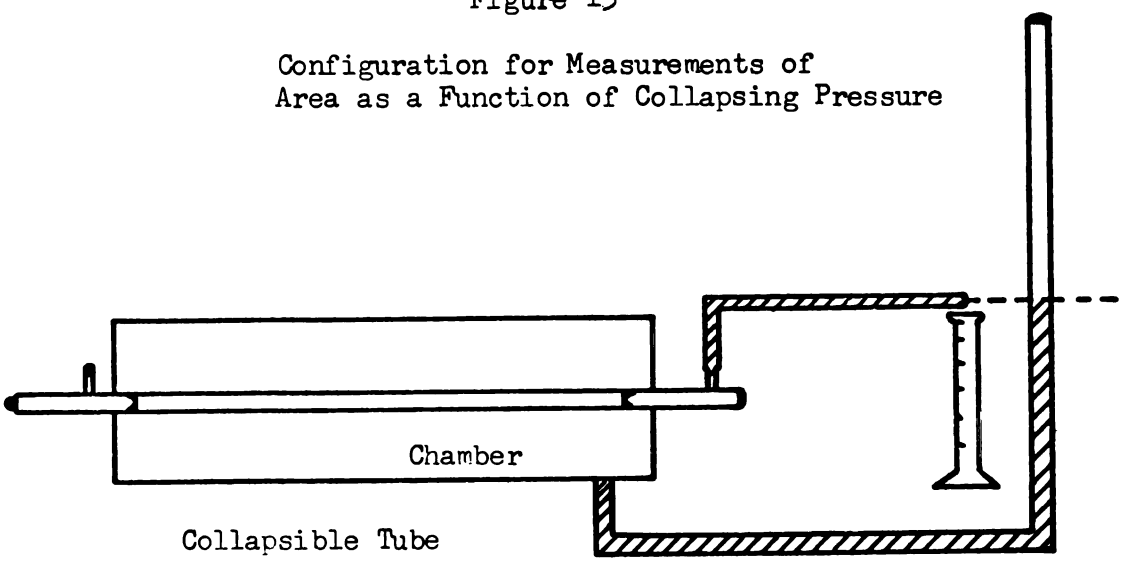

collapsible tube is measured. This procedure was repeated and found to be reproducible within ± 0.2 cm^3 for any given pressure.

The open loop and closed loop responses are measured with almost the same system. The only difference is that for open loop response, P_2 and P_c are varied independently, and for closed loop response, $P_s = P_c$ and P_2 is related to P_s by $P_2 = P_s - R_sQ$. Figure 16a shows the system in closed loop configuration and Figure 16b shows the loop open with independent inputs. Figure 17 shows the apparatus for measurement of open loop characteristics.

Figure 16 Open and Closed Loop Configuration

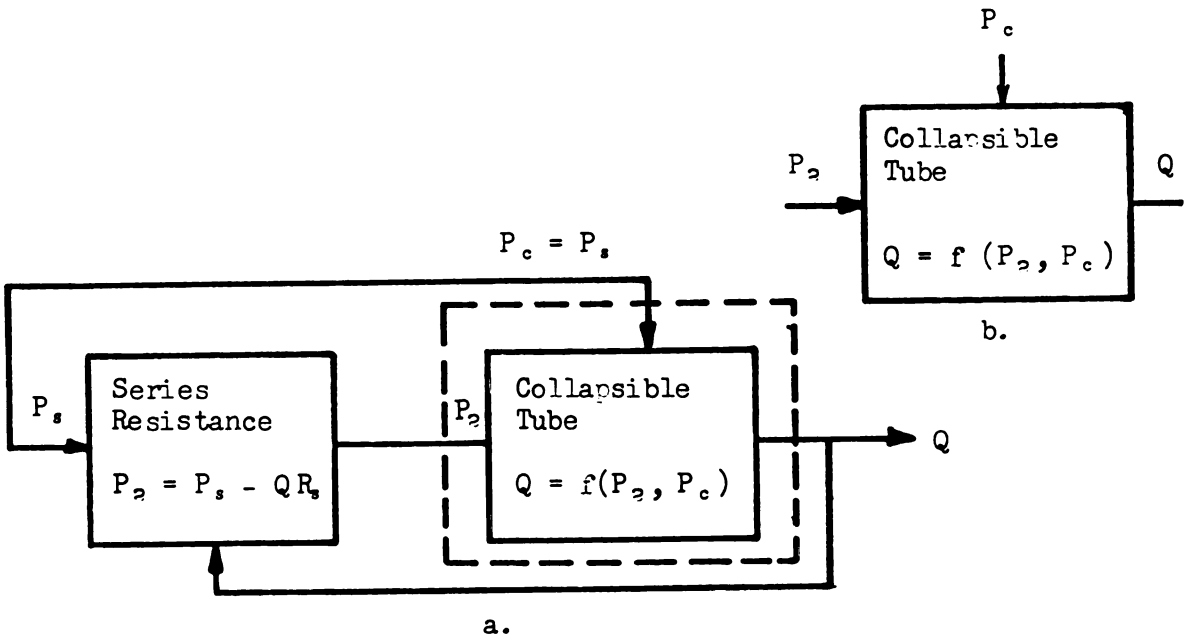

Figure 17 Apparatus for Measurement of Open Loop Characteristics

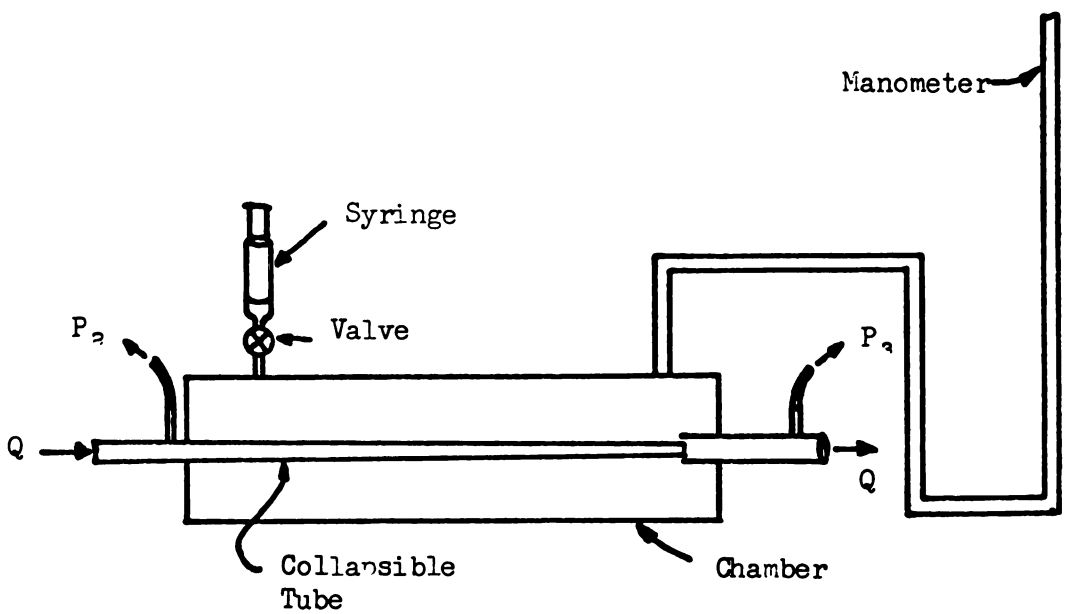

Results and Discussion

The "equation of state" as used in the theory (page 22) is an empirically derived equation based on measurements of the area of the collapsible tube portion of the hydraulic test section. As the collapsible tube is made to change area by application of a pressure difference across the walls, the cross-section changes shape from a circle to an ellipse of increasing eccentricity to a complicated geometry of a double ellipse, and ends as two circles connected by a fully collapsed section (see Fig. 18).

Figure 18

Cross Section of Collapsible Tube as a Function of Collapsing Pressure

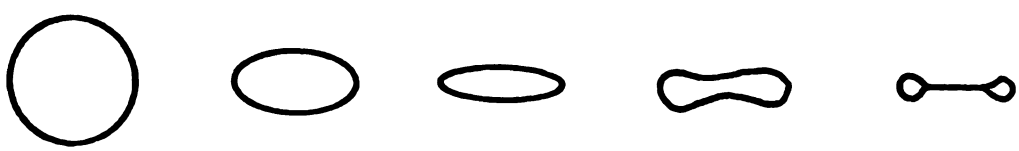

$P_c - P = 0$ (cm H_2O) $P_c - P = 2$ $P_c - P = 5$ $P_c - P = 15$ $P_c - P = 40$

The relationship between collapsing pressure and area for a $\frac{3}{8}$" penrose tube is shown in Fig. 19. This relationship is difficult to fit accurately with a polynomial. Without success, polynomials to tenth order were tried by a curve-fitting technique on an IBM 1620. It was found, however, that two decreasing exponentials and a power term could be used to fit the curve. The resulting equation of area as a function of applied pressure ($P_c - P$) is:

Figure 19

Area of Collapsible Tube as a Function of Collapsing Pressure

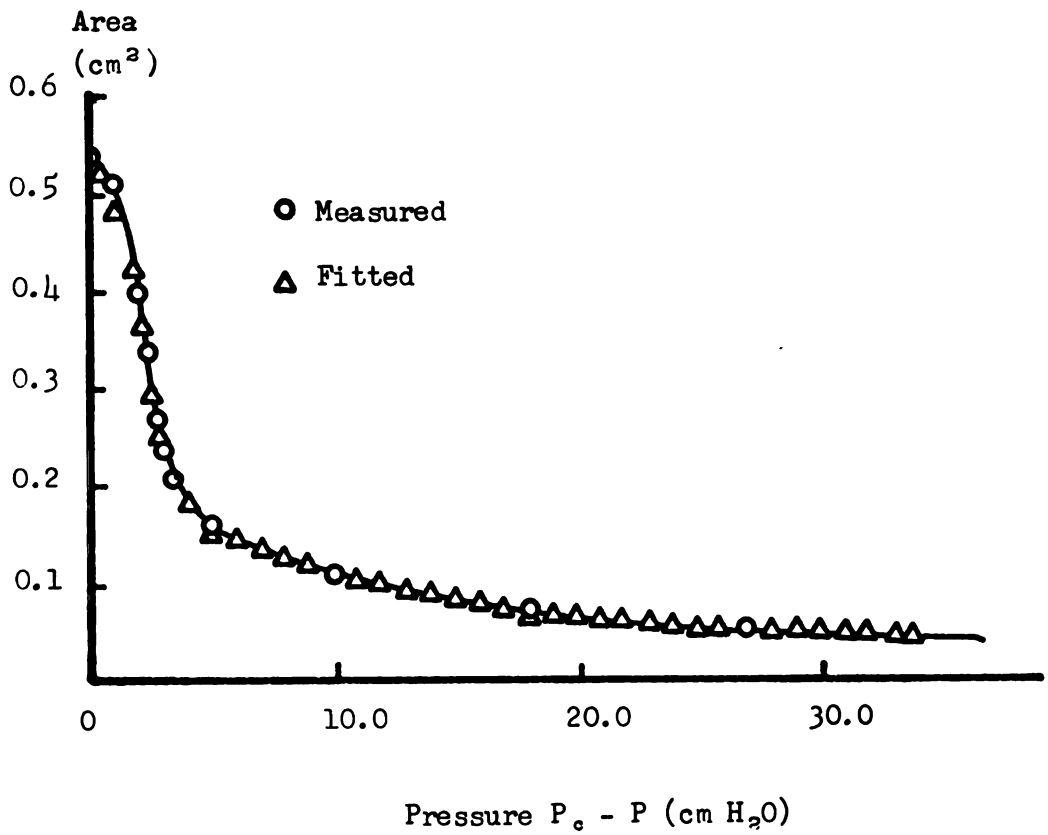

$$A = 0.362\, e^{-0.159(P_c - P)^2} + 0.105\, e^{-0.0062(P_c - P)^2} + \frac{0.398}{(P_c - P + 1)^{0.2}} + 0.03$$

The non-linear characteristics of this relationship are important to the operation of the system. As noted in the introduction, other investigators have stated that a change in the relationship between interstitial pressure and arterial pressure would have to occur at the pressures where autoregulation begins. This need not be true if the relationship between collapsing pressure and resistance of the collapsible tube is non-linear. Fig. 20 shows the open loop characteristics of the system for $\frac{3}{8}$" penrose tube and Fig. 21 shows the characteristics of a closed loop system.

Figure 20 Open Loop Results

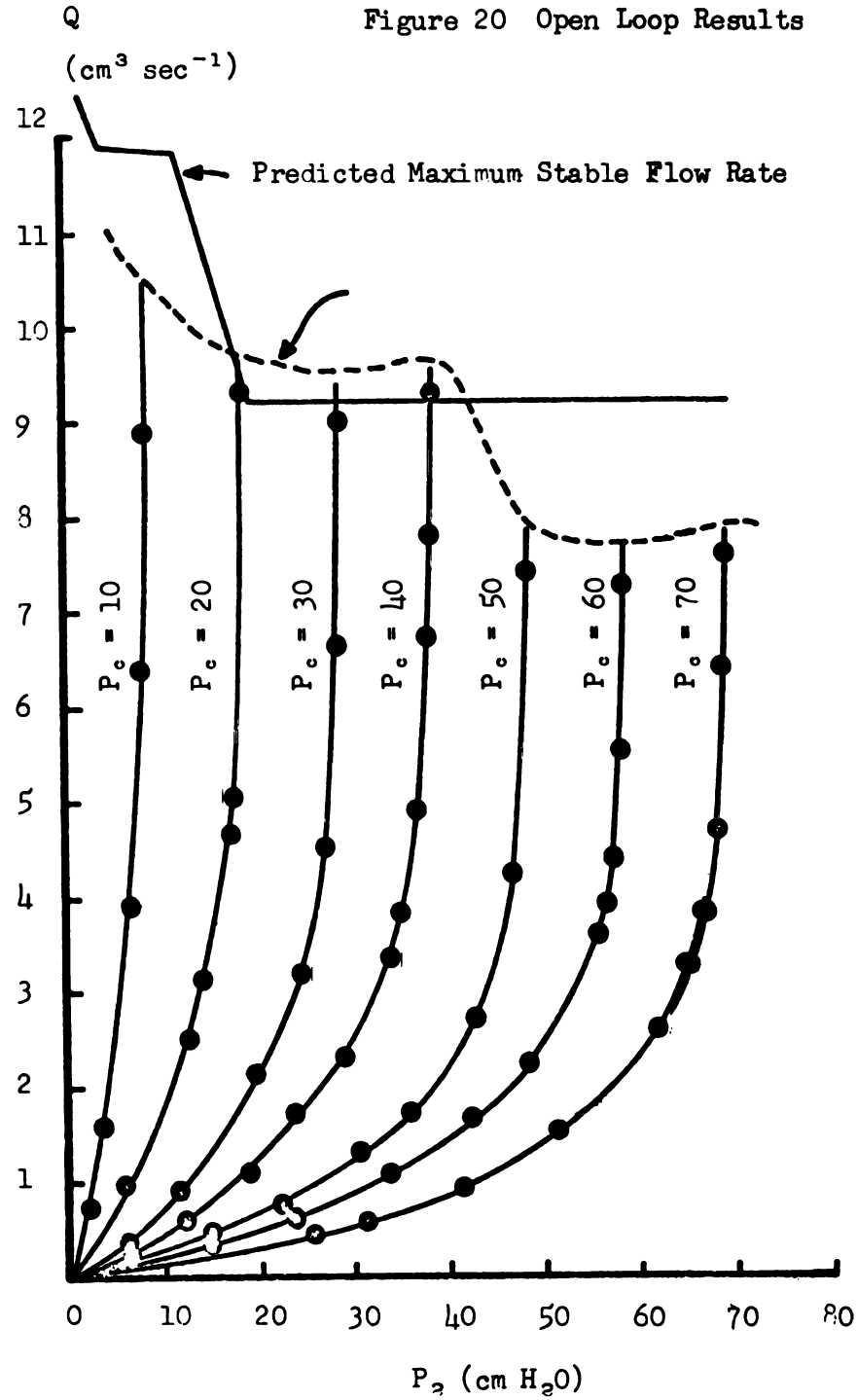

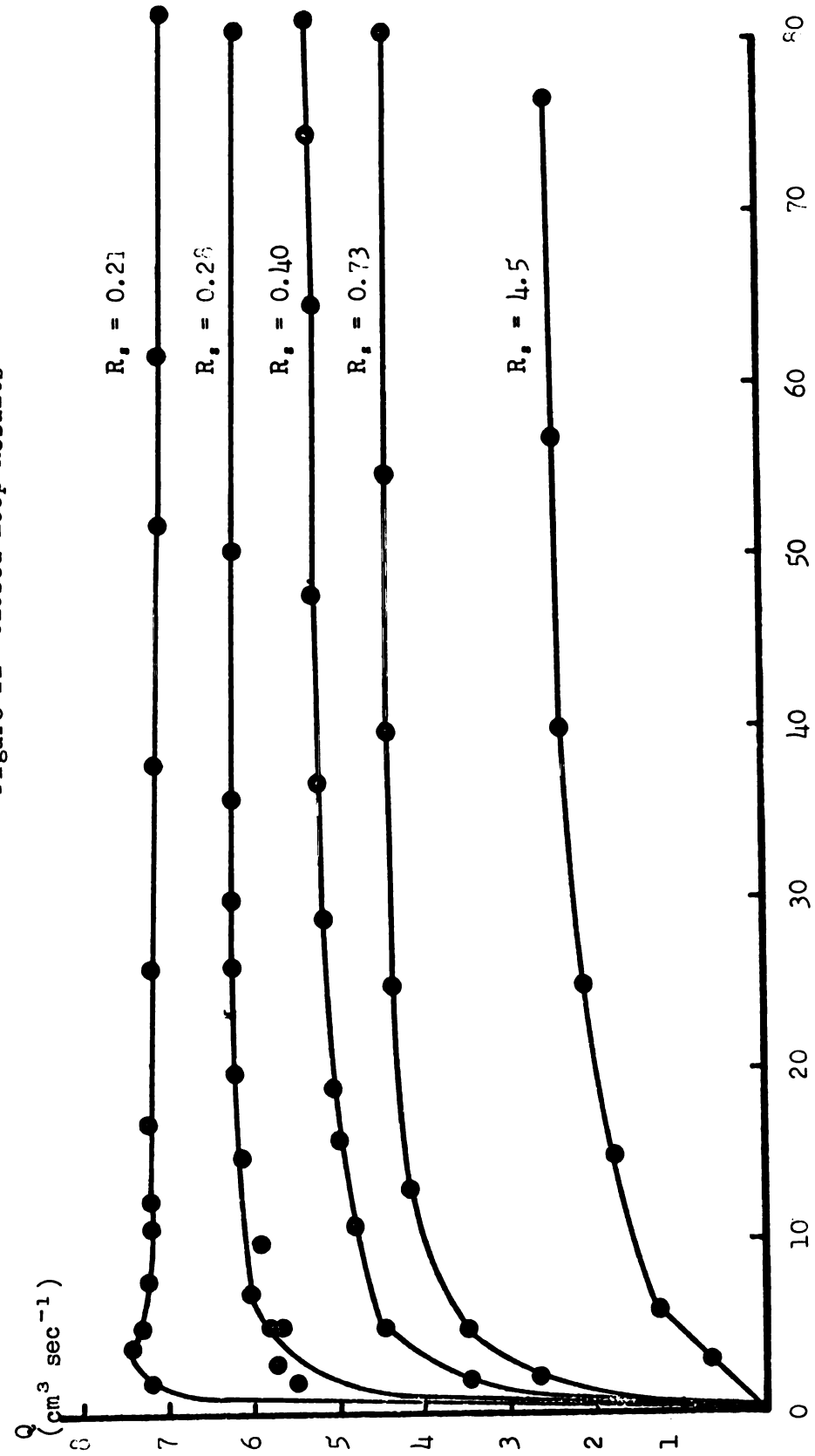

Figure 21 Closed Loop Results

Several observations can easily be made. The system in closed loop configuration can regulate quite well (Fig. 21). In fact, using the proper materials and values of the series resistance, the system has application as a fluid flow controller. This control is accomplished passively with a fixed relationship between input pressure and collapsing pressure determined by the input resistance $R_{\emptyset}$, the series resistance (R_s), between the leak point and the collapsible tube and the flow (Q). The difference in results between open loop and closed loop systems emphasizes the importance of the resistance to fluid flow between the cardiovascular system and the interstitial space. The dependence of the shape of the closed loop control curve on R_s is also important. When the difference in viscosity between blood and water is accounted for, it can be seen that for a certain value of R_s regulation will not occur within pressure ranges studied in the cardiovascular system. This is significant when one considers that the series resistance in the kidney contains the efferent arterioles which can be affected by a wide variety of drugs and the autonomic nervous system. Further analysis shows that the input resistance, $R_{\emptyset}$, can also affect regulation. If $R_{\emptyset}$, represented by afferent arterioles and small arteries in the kidney is high, much of the pressure will be lost before reaching the venous circulation. Since the relationship between pressure and resistance in the venous circulation is non-linear, different operating characteristics are found at a lower venous pressure.

It can be seen from the theoretical development and from direct measurements in a hydraulic test section designed to simulate the renal

blood flow control mechanism, which parameters can be expected to affect regulation if, indeed, the postulated model does represent actual renal hemodynamics. Although it is postulated that the autoregulatory resistance change occurs in the venous circulation, the form of this regulation (shape of the pressure-flow curves) is affected by preglomerular resistance, efferent arteriolar resistance, capillary permeability and venous collapsibility.

The oscillatory behavior of the system is shown in Fig. 22. This is the simplest mode of oscillation showing an equilibrium flow of 9.5 cm^3 sec^{-1} with an amplitude of ± 3.5 cm^3 sec^{-1} and a frequency of 2.8 Hz. The flow is leading the pressure with a phase shift of 26°.

IV. Experiments on Dog Kidneys

Observations were made on the kidney for three purposes: (1) to find the section of the renal circulation in which blood flow control occurs, (2) to describe the pressure distribution in the renal vein, and (3) to compare regulation in the venous circulation with the mathematical model predictions.

Methods

Experiments were run on eight kidneys of one year old dogs ranging from 25-30 kg. The dogs were anesthetized with sodium pentobarbital at a dose of 30 mg. per kg. of body weight and the kidney exposed through a retroperitoneal flank incision. The renal artery and vein were isolated with a minimum of manipulation. After the preparation was completed, the dog was given 4 mg. of heparin per kg. of body weight and 5 mg. per hour thereafter.

Renal artery pressure was measured from a needle in the renal artery and renal arterial blood flow was measured with an appropriately sized electromagnetic transducer of the same type used in the model measurements (page 41). Venous pressure at the renal vein and within the kidney was measured by retrograde insertion of a drawn polyethylene cannula.

Polyethylene tubes of various sizes were drawn in air over a small electric heater to tip sizes ranging from 0.1 mm to 0.7 mm and inserted through a needle fixed in a rubber tube inserted into the renal vein, taking care not to wedge the cannula. Although this technique has been in use for some time by other investigators (Hinshaw, 1963, 1964) and

would seem to be almost routine, some difficulty was encountered in obtaining a cannula that had a small enough tip to pass into the deep venous circulation and still have enough structural ridigity to prevent it from folding over in a small vein. A great many sizes of tube can be drawn to a still greater variety of tip sizes all of which can be passed into the renal venous circulation. The criterion used for satisfactory placement of the cannula was a recording of a high pressure just before wedge. As venous pressure increases in a rather smooth exponential for the first 40-50 mm up the venous circulation, the arbitrary decision of accepting a particular pressure, obtained with a given cannula, is difficult. If the cannula is not placed deeply enough, the resistance changes will be upstream from the measurement point. By using a slightly smaller cannula, the resistance changes will occur downstream of the measurement point. Using a smaller cannula presents another difficulty. If the tip is too fine, it will invariably bend over and the folded tube inserted to the wedging point. Also, with too small a cannula, it is almost impossible to detect wedging of the tip.

Pressure and flow were measured with the same instruments used to measure the same variables on the mechanical test section (see page 41). Hydraulic occluders (Jacobson and Swan, 1966) were used on the aorta upstream and downstream with respect to the kidney to vary renal arterial pressure.

Certain objections to direct measurement of pressure within small renal veins by means of retrograde insertion of a cannula have been brought forward by Haddy (1965). Haddy has pointed out that it is impossible to calculate the actual values of resistance of segments of

small veins. This is because of the fact that flow within the vein at the site of pressure measurement is not known. This observation is certainly correct. In order to calculate the resistance of the segment of small vein, one would have to assume that flow is uniform in all the parallel veins and know the total number of veins which shared the flow measured at the renal artery. This assumption is not necessary in the case where the only information sought is whether the resistance changed upstream or downstream of the catheter tip. The only way that such calculations could be improperly based would be if flow through the particular vein containing the cannula decreased when perfusion pressure increased.

Although this specific reaction is quite unlikely, another artifact can occur if the cannula is blocking flow as also mentioned by Haddy. If there are very few side branches interconnecting the interlobular veins and flow is blocked, it is possible to measure capillary, even, arteriolar pressure with a cannula in a vein. That this is very unlikely in the case of interlobular pressure measurements can be seen by inspecting Figure 31. It can be seen that the slope of the curve relating deep venous pressure to distance within the kidney is constant near the deepest pressure measurement. This indicates that resistance per unit length is constant, which is likely because of the almost constant cross section found in that segment of the circulation, or that cannula was interfering with flow in such a way that resistance per unit length appeared exactly constant.

Also, if the cannula were wedged into the vein preventing flow, the measured pressure would not increase with distance but would re-

main constant. If the cannula were influencing flow, a bend toward the pressure axis would be evident at the deepest measurement. It is also unlikely that all measurements were taken just at the wedge point because the cannula was withdrawn slightly from the point of maximum insertion.

Results and Discussion

Data from the kidney studies are tabulated in Appendix D and plotted in Figures 24-31. In each figure, the curve marked "A" is the pressure-flow diagram of the entire renal circulation while "B" and "C" are pressure-flow diagrams of the circulation before and after the interlobular veins respectively. Autoregulation is shown in pressure-flow curves by a change in slope. If the change is toward the pressure axis, it indicates an increase in resistance to maintain constant flow. Location of autoregulation in the arterial or venous circulation can be done by inspecting curves "B" and "C" to see which has the greater change in slope. Each of the kidneys exhibits autoregulation, and in each kidney the regulation occurs downstream of the deep-venous pressure measuring point. In Figures 23b-29b a slight increase in resistance is evident at the high end of the pressure range and in Figure 30b regulation is present upstream from the venous measurement point.

There is no evidence to suggest that this change in resistance, upstream of the measurement point, occurs in the arterioles. In each measurement it was noted that if the venous cannula was not placed far enough into the venous circulation, the resistance change responsible for regulation was upstream from the point of measurement. When a

Figure 23

Segmental Pressure-flow Curves - Kidney I

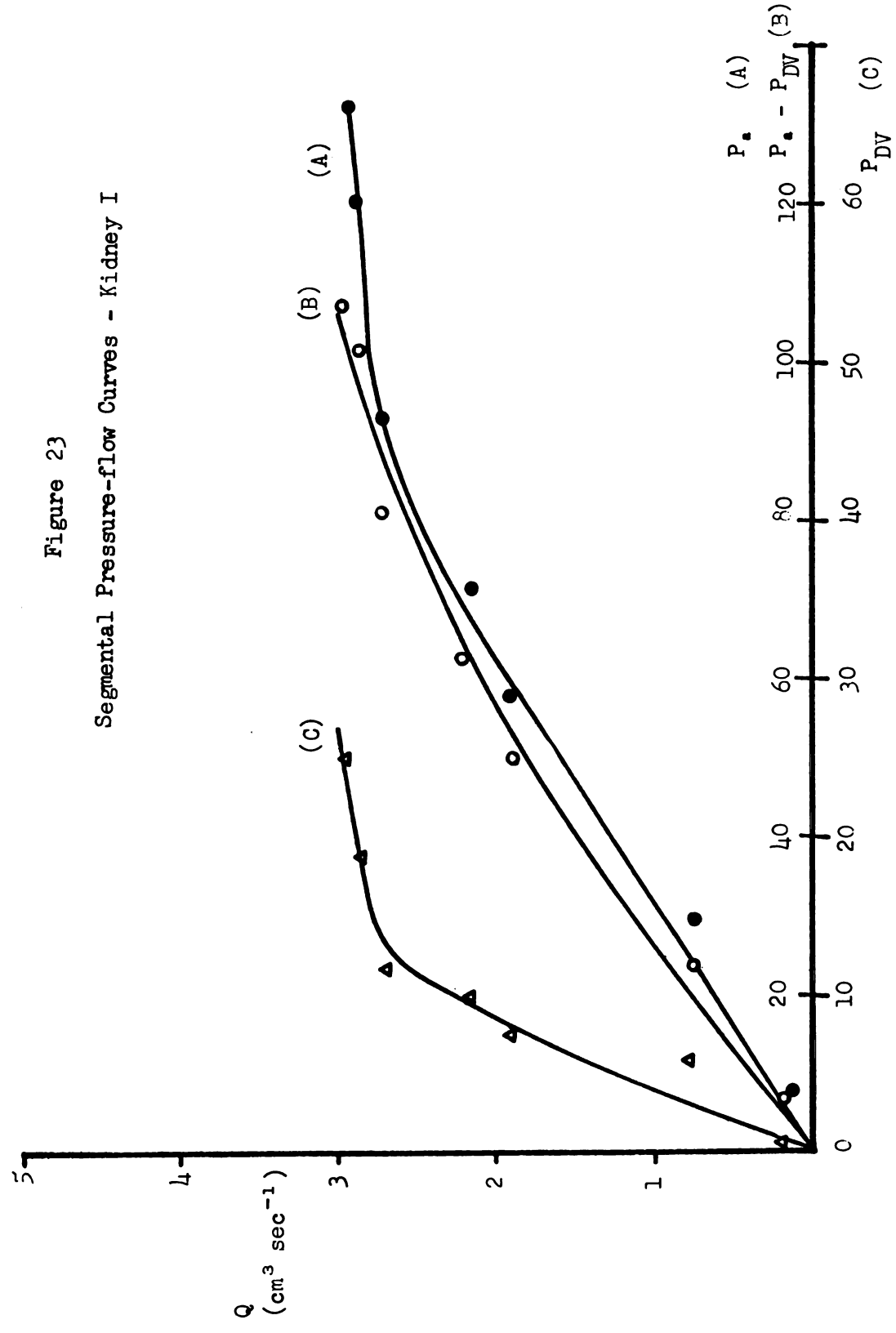

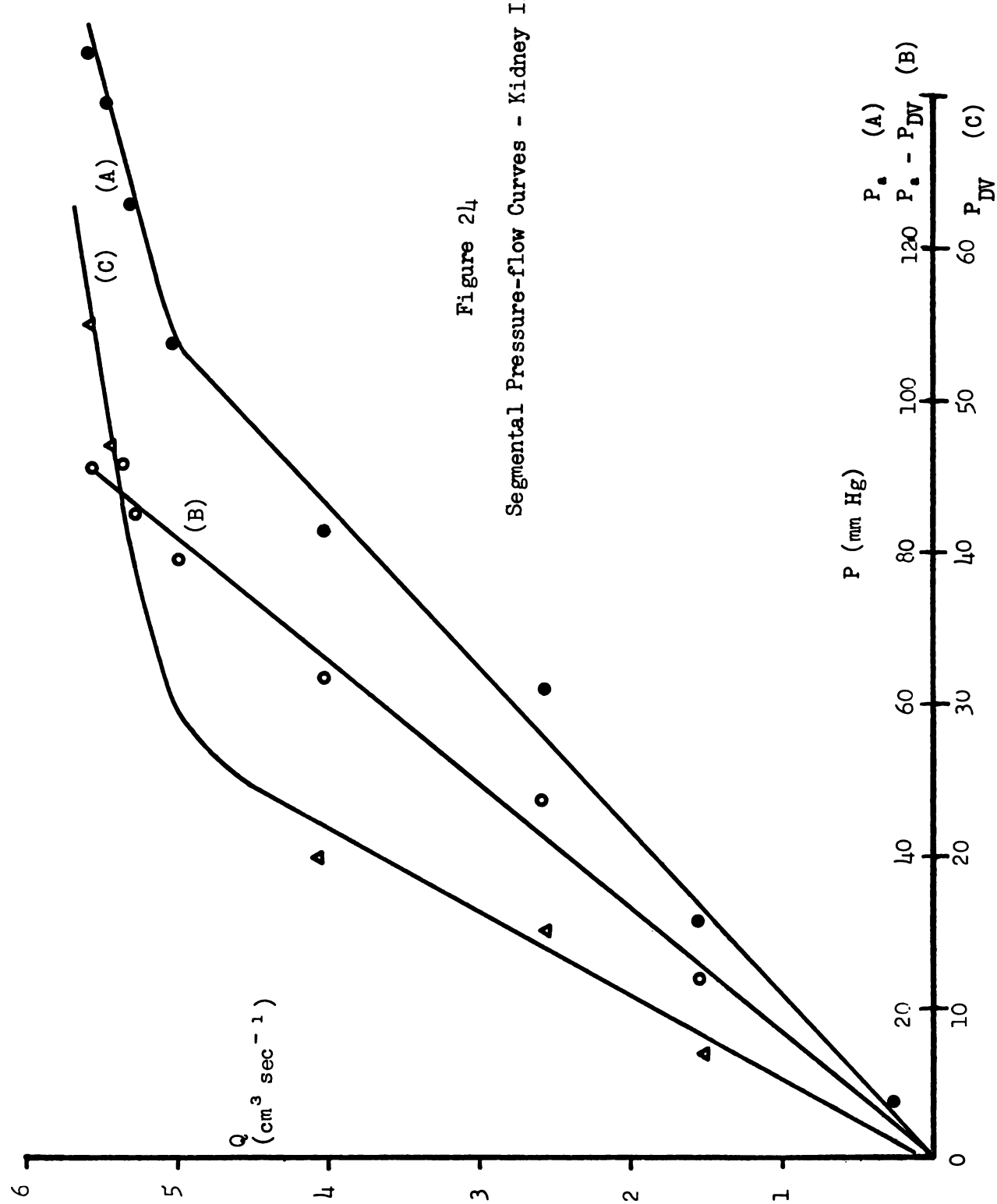

Figure 24

Segmental Pressure-flow Curves - Kidney II

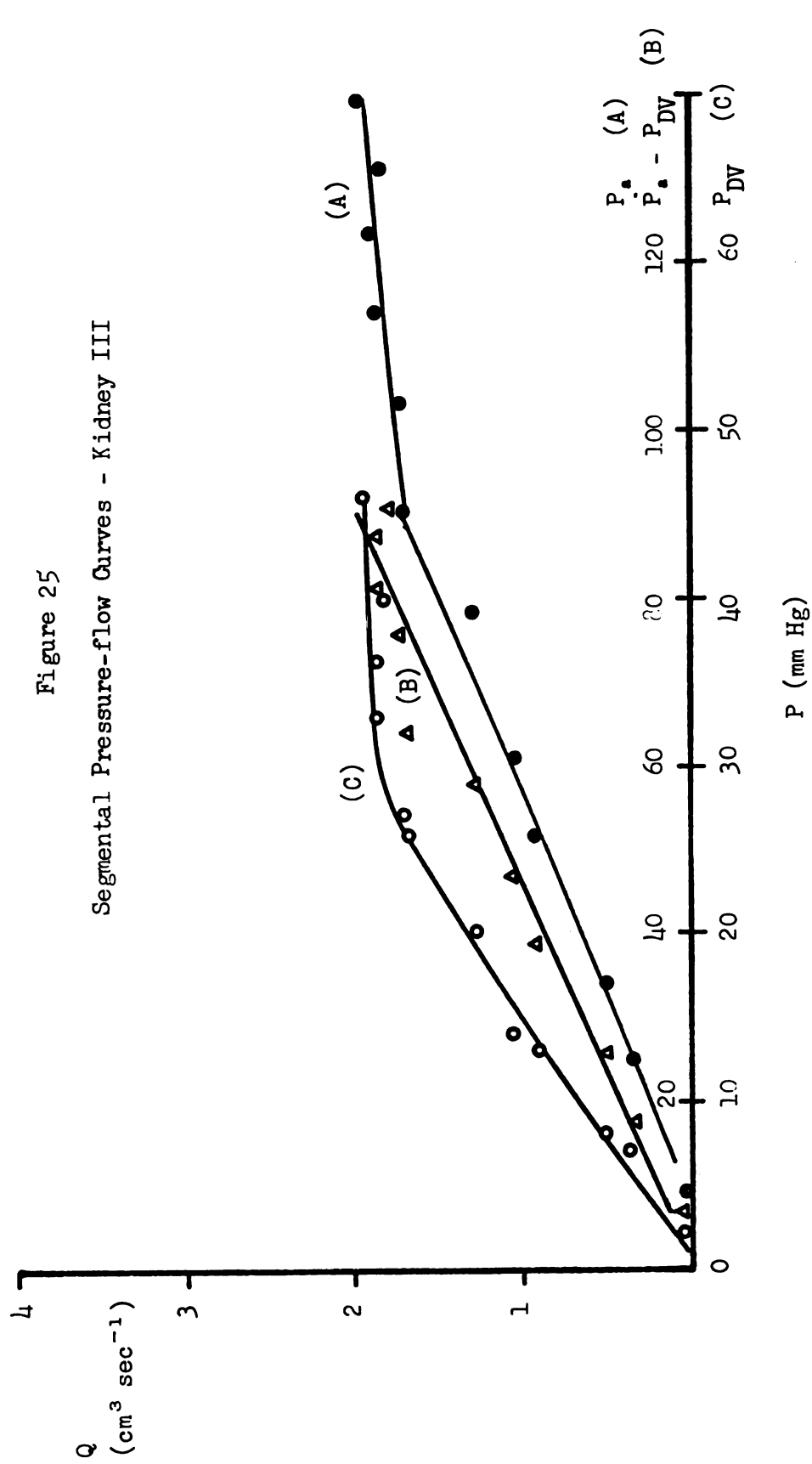

Figure 25

Segmental Pressure-flow Curves - Kidney III

Figure 26

Segmental Pressure-flow
Curves - Kidney IV

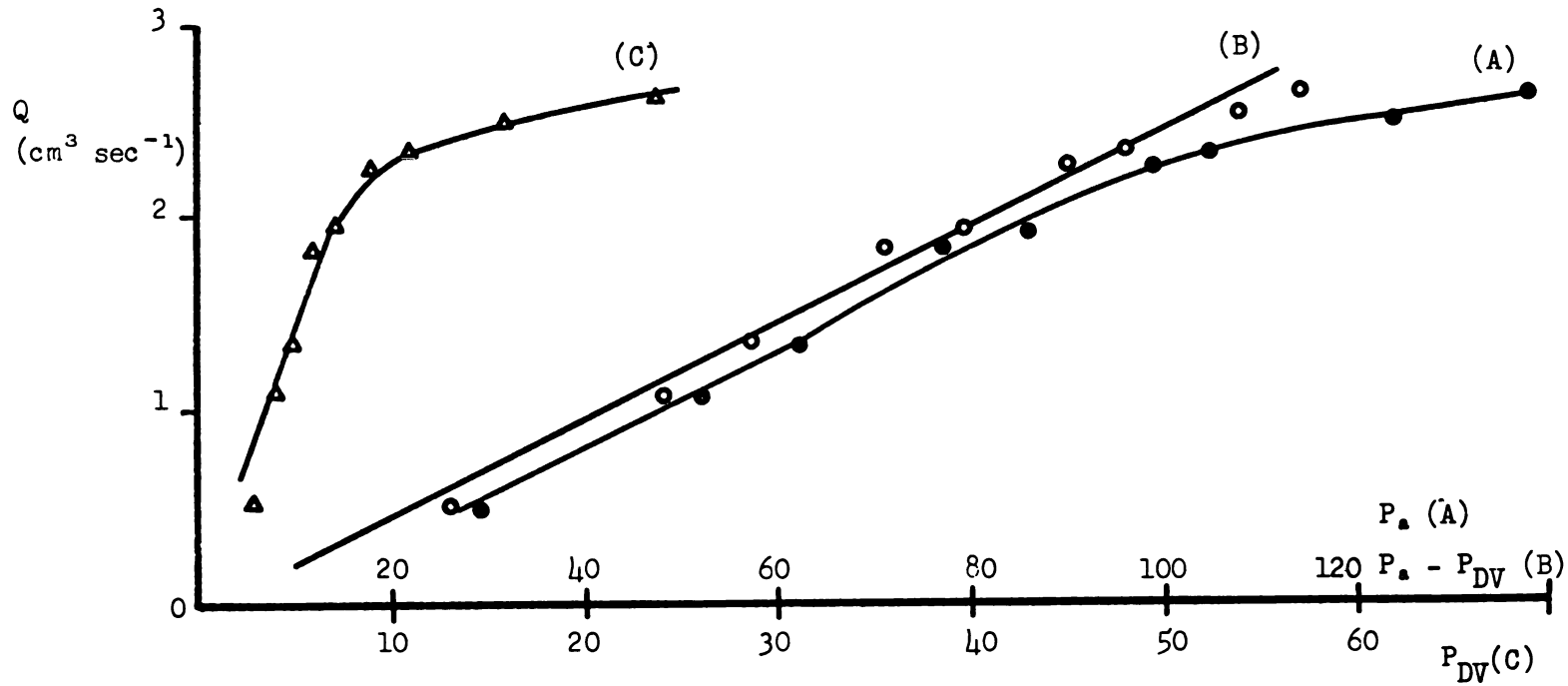

Figure 27

Segmental Pressure-flow Curves - Kidney V

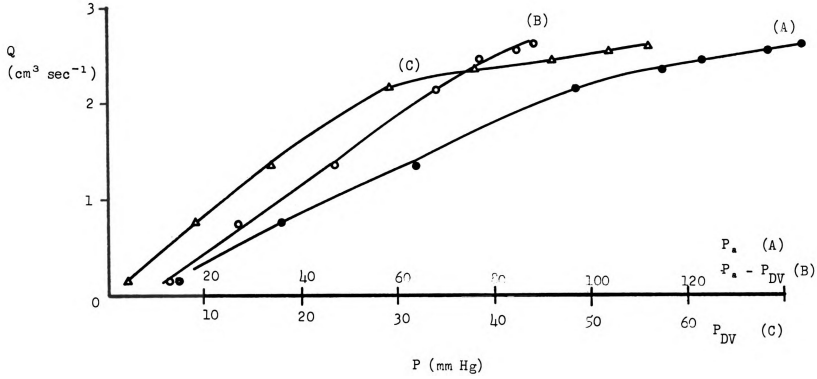

Figure 28

Segmental Pressure-flow Curves - Kidney VI

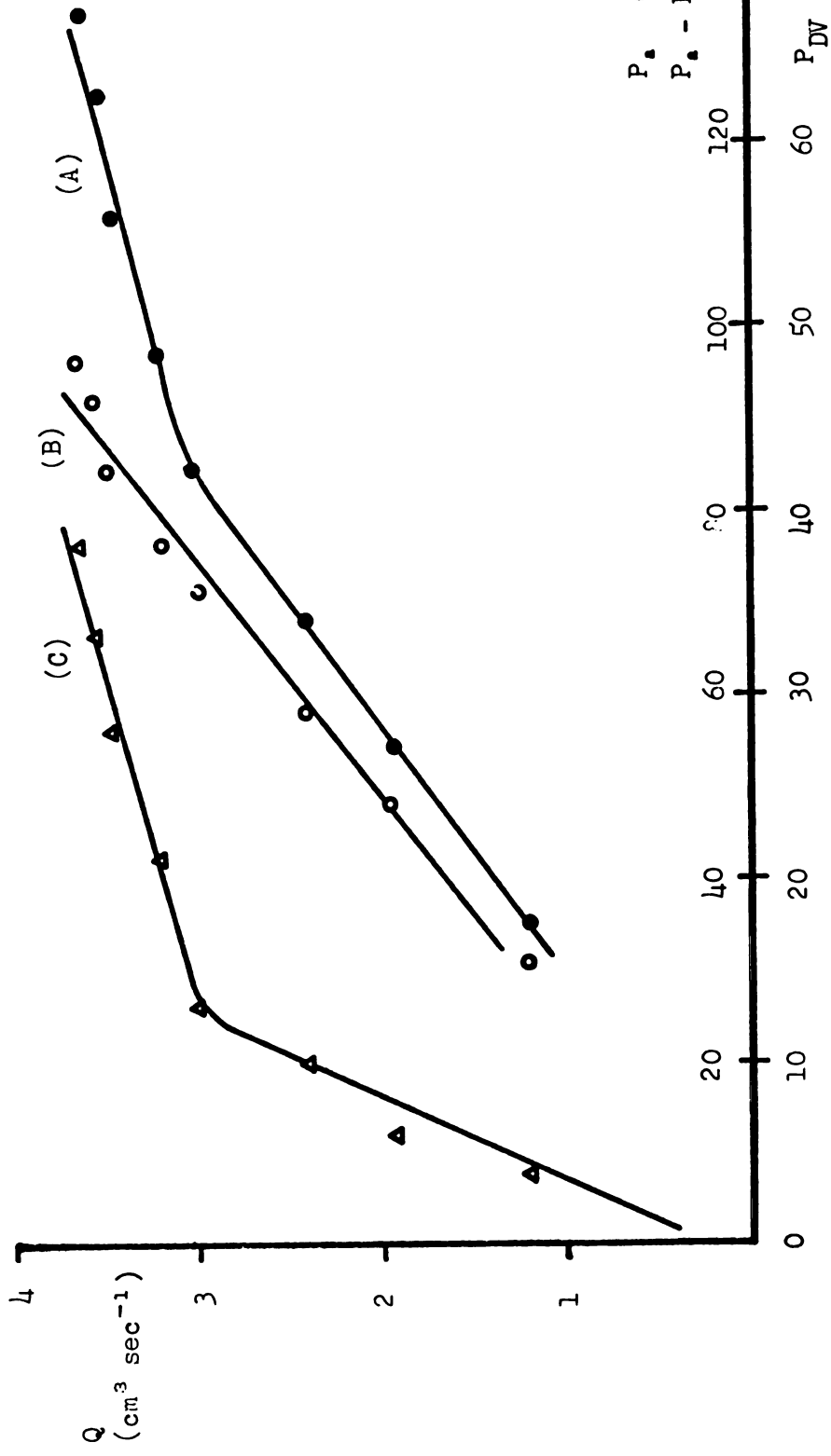

Figure 29

Segmental Pressure-flow Curves - Kidney VII

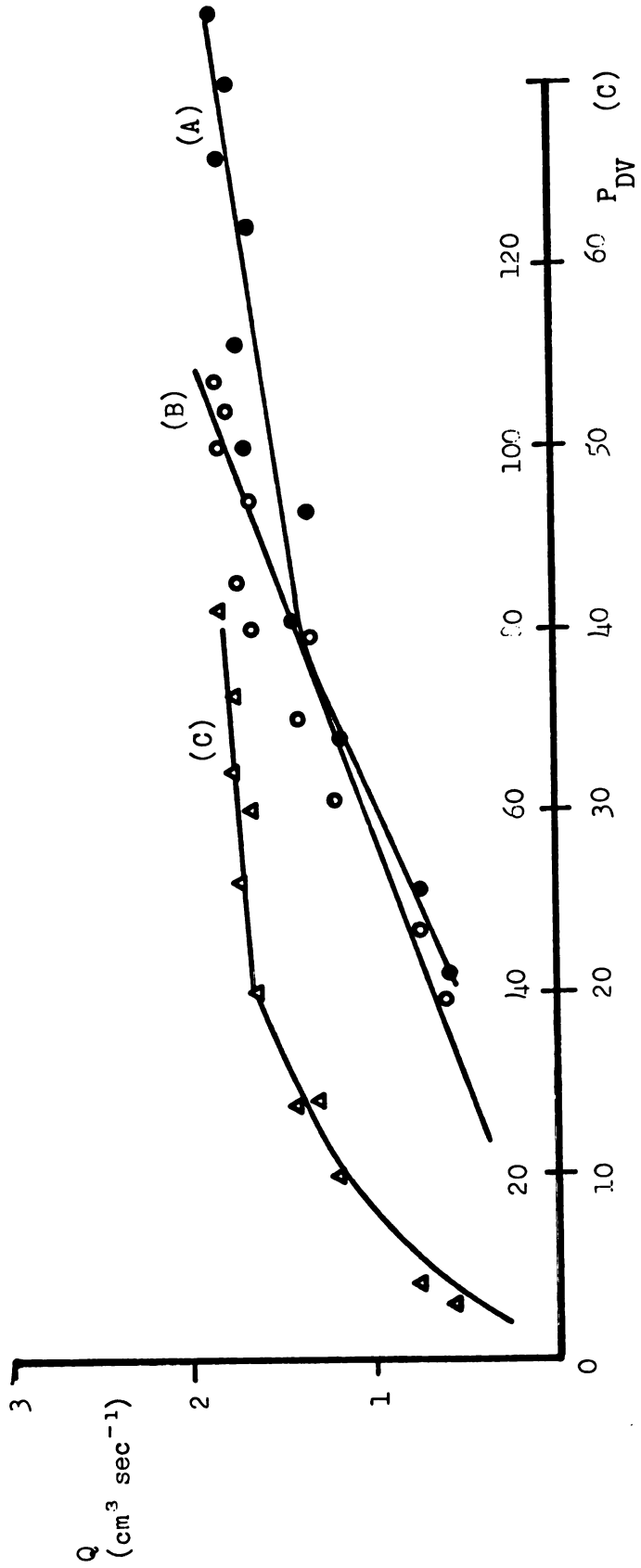

Figure 30

Segmental Pressure-flow Curves - Kidney VIII

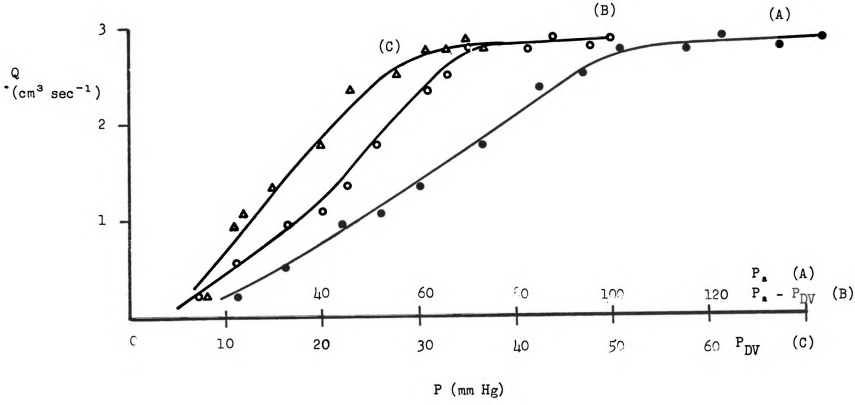

Figure 31

Pressure Distribution in the Renal Vein

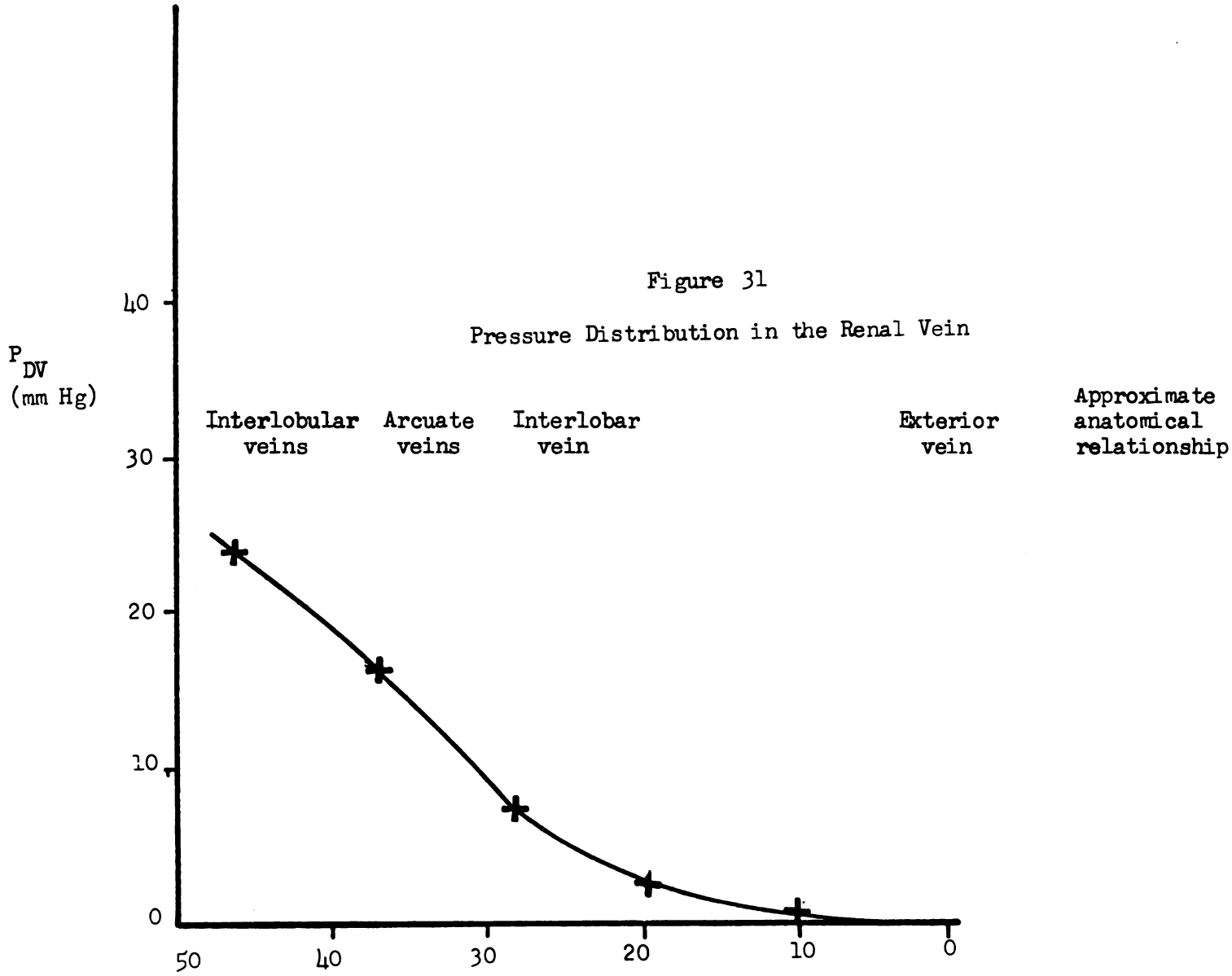

smaller cannula was substituted, the resistance change was downstream from the measurement point. This suggests that the slight changes in resistance upstream of the interlobular veins seen in the first seven kidneys are still in the venous circulation but above (upstream of) the position of the cannula, and, in kidney VIII, it probably was not possible to work the cannula in far enough. Therefore, all the resistance would occur downstream of the measurement point if a cannula could be made to pass far enough into the interlobular veins.

Some comparisons can now be made between the regulation predicted by the mathematical model and the regulation measured in the mechanical model and kidney. From Figure 6 it can be seen that the initial slope of the pressure-flow diagram and the maximum flow rates are dependent on the series resistance (R_s). R_s is identified exactly in the mathematical and mechanical models as the resistance between the point where pressure is fed forward to collapse the thin-walled tubing, and the beginning of the collapsible tube (See Figs. 1 and 3). The analogous series resistance in the kidney (Fig. 1 and Table II) must be more vaguely described. The section of the renal circulation representing R_s is the section between the distributed site of tissue fluid formation and the beginning of the collapsible veins. Resistance of the efferent arterioles and part of the peritubular capillaries, and permeability of filtration membranes, proximal tubules, and peritubular capillaries can all be parts of the series resistance. Unfortunately it is difficult to assess the contribution of any of these possibilities except to note that the efferent arterioles have a high vasomotor reactivity.

Without being able to identify R_e structurally with precision within the kidney, it can still be identified functionally. In order to compare pressure-flow curves from the model to the curves from the kidneys, a correction must be made to account for the difference between the viscosity of blood and of water. In hydrodynamics, flow characteristics are usually expressed in terms of the Reynolds number which is a function of viscosity (Prandl and Tietjens, 1934; Schlichting, 1960). If this expression had been used, it would be apparent that the pressure-flow curves predicted by the model for $R_e > 5.0$ (Fig. 6), measured in the hydraulic test section with $R_e > 4.5$ (Fig. 21), and measured in the kidney (Figs. 23a-29a) would have the same form. The use of a dimensionless quantity such as the Reynolds number would have made it difficult for physiologists to compare the kidney results with those of other investigators. To make a comparison between model curves and kidney curves, it is necessary, therefore, to multiply the pressure in the model curves by four (μ blood = 4 μ water).

The conclusion that can be drawn from the pressure-flow curve comparison is that the series resistance in the kidney is probably higher than the uncollapsed venous resistance. This conclusion must be qualified because the collapsibility of the penrose tubing used is much higher than that of the small renal veins. Collapsibility is a function of both wall structure and radius of the vessel. The difference in wall elasticity between interlobular veins and penrose tubing is not easily measured, but the veins are certainly smaller than the smallest penrose tubing available. Because collapsibility varies as the cube of the radius, greater regulation is expected using penrose

tubing in the test section.

A similar comparison can be made between the computer predictions for pressure distribution along the collapsible tube (Fig. 10) and measurement of venous pressure as a function of distance along a venous vessel within the kidney (Fig. 31). The pressure distribution is also affected by R_e and the model also predicts that the series resistance in the kidney is high compared to the uncollapsed venous resistance.

Some investigators have made a few intuitive guesses of how the renal blood flow control system would work if it operated on a "tissue pressure" principle. The mere existence of the mathematical and mechanical models is enough to show that these attempts at theory were misguided. Swann (1964) and Winton (1964) have stated that a passive mechanism could not explain autoregulation because interstitial pressure increases proportionately with arterial pressure. They have stated that a disproportionate increase in interstitial pressure relative to arterial pressure would be required to collapse the renal veins significantly in the pressure range in which autoregulation occurs. Without a model or physical description they did not realize that their "criteria" would only hold if the area of the collapsible veins were a linear function of collapsing pressure. This linearity cannot exist in a geometry of a collapsing tube as shown in Appendix A.

Johnson (1964) stated that autoregulation should not be abolished by agents which paralyze vascular smooth muscle. He was not aware of (or concerned with) the effects achange in the resistance of muscular arterioles could have on passive autoregulation. Schmid and Spencer (1962) stated, "The linearity of the (pressure-flow) relationship and

the sharp inflection of the curve...are indirect evidence against a passive mechanism." Figure 21 shows pressure-flow curves measured in a passive system made up of penrose tubing. These curves show more linearity and a sharper inflection than measured in kidneys.

Other investigators have hypothesized control functions to explain their observations that could be more easily explained by a passive control. Waugh (1964) has shown that it is possible to elicit a damped second-order response in flow to a step input of pressure. He attributed this response to a "hunting type" reaction. The same response is seen in passive svstems and depends on control loop time constants. Waugh noted that the oscillating response is abolished when renal vascular reactivity is abolished with chloral hydrate. He interpreted this as proving that the oscillations were caused by smooth muscle reactivity. Another explanation could be that by changing vascular diameter with the chloral hydrate, he changed the control loop time constants. Haddy (1965) found that renal arterial pressure increases transiently for 2-4 seconds in response to a 0.5-2 sec flow pulse. He interpreted the reaction as vasotonic, but the same reaction could occur easily in a passive system. A flow pulse forced upon a system which is designed to regulate flow can cause internal pressures to increase markedly. If the fluid transudation time constant is high or the system is surrounded by an elastic capsule, the control system can display a long time constant to equilibrium.

Regulation of GFR (Harvey, 1964; Schmid, 1964) and regulation of lymphatic pressure (Haddy, 1958a) are more difficult to explain with a passive control system. It could be that the tubules and lymphatic

vessels also regulate by collapsing just as hypothesized for the small veins.

Waugh (1964) has based many of his conclusions on his observations of deep venous pressure during autoregulation. His results show the resistance change located upstream from the catheter tip instead of downstream. One explanation is that Waugh failed to insert his cannulae far enough into the venous circulation. This can easily be done if the proper sized tubing is not chosen and proper technique is not used in drawing the tubing to correct taper.

V. Summary and Conclusions

The results of the computer solution of a mathematical model and the direct measurements on a hydraulic test section to verify the model show the existence of a possible passive mechanism for the renal blood flow control which can operate in the renal venous circulation. The model also provides an insight into the role of arterial and arteriolar resistance and capillary permeability might play in influencing this resistance.

Autoregulation of blood flow in the kidney is postulated to be caused by an increase in resistance of the interlobular and arcuate veins, caused by their collapse with increasing arterial pressure. The cross-sectional shape of these veins is a function of their structure and collapsing pressure. Collapsing pressure, in turn, is the difference between pressure at the site of formation of interstitial fluid and pressure within the collapsing vein. At a given blood flow rate, the magnitude of the collapsing pressure depends on the resistance (R_s) of the segment between the site of formation of interstitial fluid and the collapsing veins. Any factor which can effect R_s can change the regulation characteristics of the collapsible veins. Because the relationship between resistance of the collapsible veins and the absolute magnitude of the collapsing pressure is non-linear, and because the drop in pressure across the small arteries and preglomerular arterioles determines the pressure at the site of formation of interstitial fluid, the resistance (R_a) upstream of the leak point affects regulation.

Other factors predicted to influence autoregulation include ca-

pillary permeability and collapsibility of the veins. Capillary permeability influences regulation time constants and series resistance. Collapsibility of the veins is a function of both stiffness and radius. As the vein size increases from the venules to renal vein, the collapsibility as a function of radius increases. But, as they become larger, the wall thickness increases and they become stiffer, decreasing collapsibility. Collapsibility is a function of distance along the venous circulation and has a maximum somewhere between the ends.

Measurement of renal arterial pressure, blood flow rate, and deep venous pressure within the dog kidney support earlier findings (Hinshaw, 1964) that the site of autoregulation resistance changes is in the interlobular or deep arcuate veins.

The findings indicate that the principle mechanism of renal autoregulation is a passive collapse of interlobular veins. This passive type of control is very sensitive to changes in resistance upstream from the veins, however, and could be augmented or controlled completely by arteriolar changes, particularly efferent arteriolar changes. The model in no way proves how autoregulation works but its existence shows that a passive mechanism is possible. With a mathematical description from which to work, it may be possible to design more meaningful experiments.

Bibliography

1. Bayliss, W. M. "On the Local Reactions of the Arterial Wall to Changes of Internal Pressure," J. Physiol. (London) 28:220, 1902.

2. Berne, R. M. "Cardiodynamics and the Coronary Circulation in Hypothermia," Ann. N.Y. Acad. Sci. 80:365, 1959.

3. Bickford, R. G. and Winton, F. R. "Influence of Temperature on the Isolated Kidney of the Dog," J. Physiol. (London) 89:198, 1937.

4. Folkow, B. "Intravascular Pressure as a Factor Regulating the Tone of the Small Vessels." Acta Physiol. Scand. 17: 289, 1949.

5. Forster, R. P. and Maes, J. P. "Effect of Experimental Neurogenic Hypertension on Renal Blood Flow and Glomerular Filtration Rates in Intact Denervated Kidneys of Unanesthetized Rabbits with Adrenal Glands Demedullated," Amer. J. Physiol. 150:534, 1947.

6. Gordon, B. "Vasodilator Products in Blood Resulting from Nucleotide Breakdown in Ischemic Tissue," Intern. Congr. Physiol. Sci. 22nd. Leiden. pg. 196, 1962.

7. Haddy, F. J., Scott, J., Fleishman, M. and Emanuel D. "Effect of Change in Flow Rate Upon Renal Vascular Resistance," Amer. J. Physiol. 105-111, 1958a.

8. Haddy, F. J., Scott, J., Fleishman, M. and Emanuel D. "Effect of Change in Renal Venous Pressure Upon Renal Vascular Resistance, Urine and Lymph Flow Rates," Amer. J. Physiol. 195:97, 1958b.

9. Haddy, F. J. and Scott, J. B. "Role of Transmural Pressure in Local Regulation of Blood Flow Through the Kidney," Am. J. Physiol. 208:825-831, 1965.

10. Hartmann, H., Orskov, S. L. and Rein, H. "Die Gefassreaktionen der Niene in Verlaufe Allgemeiner Kreislauf Regulatimsvorgange," Pflueger Arch. Ges. Physiol. 238:239, 1936.

11. Harvey, R. B. "Effects of Adenosine Triphosphate on Autoregulation of Renal Blood Flow and Glomerular Filtration Rate," Circulation Research, Suppl. I to Vols. 14 and 15:1-178-1-182, 1964.

12. Hinshaw, L. B., Day, S. B. and Carlson, C. H. "Tissue Pressure as a Casual Factor in the Autoregulation of Blood Flow in

the Isolated Perfused Kidney," Amer. J. Physiol. 197: 309, 1959.

13. Hinshaw, L. B., Flaig, R. D., Logemann, R. L. and Carlson, C. H. "Mechanisms of Autoregulation in Isolated Perfused Kidney," Proc. Soc. Exp. Biol. Med. 103:373, 1960a.

14. Hinshaw, L. B., Flaig, R. D., Logemann, R. L. and Carlson, C. H. "Intrarenal Venous and Tissue Pressure and Autoregulation of Blood Flow in the Perfused Kidney," Amer. J. Physiol. 198:891, 1960b.

15. Hinshaw, L. B., Flaig, R. D., Carlson, C. H. and Thuong, N. K. "Pre- and Postglomerular Resistance Changes in the Isolated Perfused Kidney," Amer. J. Physiol. 199:923, 1960c.

16. Hinshaw, L. B. and Worthen, D. M. "Role of Intrarenal Venous Pressure in the Regulation of Renal Vascular Resistance," Circ. Res. 9:1156-1163, 1961.

17. Hinshaw, L. B., Brake, C. M., Iampietro, P. F. and Emerson, T. E. "Effect of Increased Venous Pressure on Renal Hemodyamics," Am. J. Physiol. 204(1):119-123, 1963a.

18. Hinshaw, L. B., Page, B. B., Brake, C. M. and Emerson, T. B. "Mechnanisms of Intrarenal Hemodynamic Changes Following Acute Arterial Occlusion," Amer. J. Physiol. 205L 1033, 1963b.

19. Hinshaw, L. B. "Mechanism of Renal Autoregulation: Role of Tissue Pressure and Description of a Multifactor Hypothesis," Circ. Res. 14, 15: Suppl. I, 120-131, 1964.

20. Jacobson, E. D. and Swan, K. G. "Hydraulic Occulder for Chronic Electromagnetic Blood Flow Determination," J. Appl. Physiol. 21(4):1400-1402, 1966.

21. Johnson, P. C. "Autoregulation of Intestinal Blood Flow," Amer. J. Physiol. 199:311, 1960.

22. Johnson, P. C. "Review of Previous Studies and Current Theories of Autoregulation," Circ. Res. 14, 15: Suppl. I, 2-9, 1964.

23. Koch, A. R. "Some Mathematical Forms of Autoregulatory Models," Circ. Res. 14, 15: Suppl. I, 269-278, 1964.

24. McDonald, D. A. "Blood Flow in Arteries," Edward Arnold Pub. London, 1960, pg. 282.

25. Prandl, L., Tietjens, O. B. "Applied Hydro- and Aeromechanics," McGraw-Hill Book Co., Inc. 1934.

26. Rapela, C. E. and Green, H. D. "Autoregulation of Canine Cerebral Blood Flow," Circulation Research 15 (Suppl. I): 1-205, 1964.

27. Rein, H. "Vasomotorische Regulation," Ergebn. Physiol. 32:28, 1931.

28. Replogle, C. R., Wells, C. H. and Collings, W. D. "Pressure-Flow-Distension Relationships in the Dog Kidney, Fed. Proc. 19:360, 1960a.

29. Replogle, C. R. "Pressure-Flow-Distension Relationships in the Dog Kidney, Master's Thesis, M.S.U., 1960b.

30. Schlichting, H. "Boundary Layer Theory," McGraw Hill Book Co., Inc. 1960.

31. Schmid, H. E. and Spencer, M. P. "Characteristics of Pressure-Flow Regulation by the Kidney," J. Appl. Physiology 17:201-204, 1962.

32. Schmid, H. E., Garrett, R. C. and Spencer, M. P. "Intrinsic Hemodynamic Adjustments to Reduced Renal Pressure Gradients," Circ. Res. 14, 15: Suppl. I, 170-177, 1964.

33. Scott, J. B., Daugherty, R. M., Dabney, J. M. and Haddy, F. J. "Role of Chemical Factors in Regulation of Flow Through Kidney, Hindlimb, and Heart," Am. J. Physiol. 208:813-824, 1965.

34. Selkurt, E. E. "Relationship of Renal Blood Flow to Effective Arterial Pressure in the Intact Kidney of the Dog," Amer. J. Physiol. 147:537, 1946.

35. Semple, S. J. G. and De Wardener, H. E. "Effect of Increased Renal Venous Pressure on Circulatory "Autoregulation" of Isolated Dog Kidneys," Circ. Res. 7(4):643-648. 1959.

36. Shapiro, A. H. "Compressible Fluid Flow," Vol. I. New York: The Ronald Press Co., 1953.

37. Stedman, C. K. "Alternating Flow of Fluids in Tubes," Statham Inst. Notes No. 30, 1956.

38. Swann, H. G. "Discussion in Hinshaw, L. B.: Mechanics of Renal

Autoregulation: Role of Tissue Pressure and Description of Multifactor Hypothesis. Circ. Res. 14, 15: Suppl. I, 120-131, 1964.

39. Torrance, H. B. "Control of the Hepatic Arterial Circulation." J. Roy. Coll. Surg. Edinb. 4:147, 1958.

40. Unna, K. "Arterieller Druck und Nierendurchblutung," Pflueger Arch. Ges. Physiol. 235:515, 1935.

41. Venard, John K. "Elementary Fluid Mechanics," (Third Ed.). New York: John Wiley & Sons, 1957.

42. Waugh, W. H. "Myogenic Nature of Autoregulation of Blood Flow in the Absence of Blood Corpusles," Circ. Res. 6:363-372, 1958.

43. Waugh, W. H. and Shanks, R. G. "Cause of Genuine Autoregulation of the Renal Circulation," Circ. Res. 8:871-888, 1960.

44. Waugh, W. H. "Circulatory Autoregulation in the Fully Isolated Kidney and in the Humorally Supported, Isolated Kidney," Circ. Res. 14, 15: Suppl. I, 156-169, 1964.

45. Wells, C. H. "Estimation of Venous Resistance and their Significance to Autoregulation in Dog Kidneys," Master's Thesis, M.S.U., 1960.

46. Winton, F. R. "Intrarenal Pressure and its Variations Due to Cooling and "Reducing" the Isolated Kidney of the Dog," J. Physiol. (London) 82:27P, 1934.

47. Winton, F. R. "Intrarenal Pressure and Blood Flow," In Transactions Third Conference, Renal Function New York, Josiah Macy, Jr. Foundation, p. 51, 1951.

48. Winton, F. R. "Pressures and Flows in the Kidney," In Modern Views on the Secretion of Urine, Cushny Memorial Lectures, London, J.and H. Churchill, Ltd., p. 61, 1956.

49. Winton, F. R. "Arterial, Venous, Intrarenal, and Extrarenal Pressure Effects on Renal Blood Flow," Circ. Res. 14, 15: Suppl. I, 103-109, 1964.

Appendix A

In this section the pressure-flow relationship for fluid flowing in elliptical tubes is derived. It is shown that for an elliptical tube $r \approx \frac{r'(A')^3}{A^3}$ where "r" is the resistance per unit length and "A" is the area.

A thin shell of fluid in a circular tube is shown below. The velocity (v) is parallel to the axis (x) of the tube and is a function

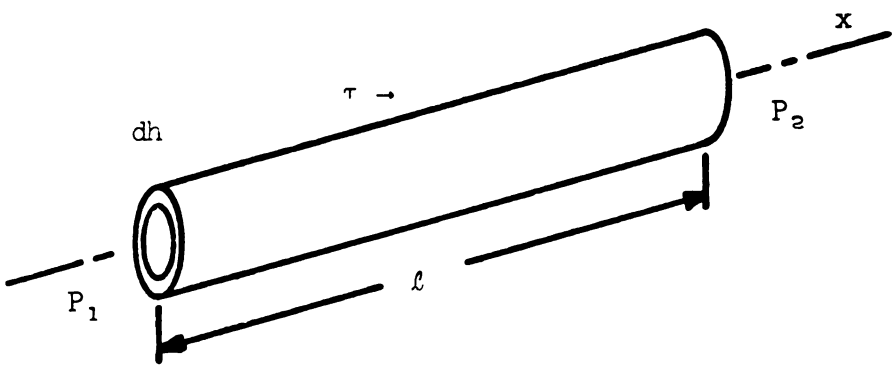

of the distance (h) from the axis. The shearing stress (τ) on the inner surface is (assuming laminar flow), $\tau_i = \mu \frac{\partial v}{\partial h}\Big|_{\ell}$, where μ is the viscosity. The stress on the outer surface is $\tau_o = \mu \frac{dv}{dx}\Big|_{h + dh}$. Expanding τ_o in a Taylor series about h,

$$\tau_o = \mu \frac{\partial v}{\partial h}\Big|_h + \frac{\partial}{\partial h}\left(\mu \frac{\partial v}{\partial h}\right) dh.$$

The net axial shearing force is

$$dF = 2\pi h \ell (\tau_i - \tau_o).$$

Substituting for τ and expanding the derivative,

$$dF = - 2\pi h \ell \mu \frac{\partial^2 v}{\partial h^2} dh.$$

This force must be balanced by the net axial pressure force. That is,

$$(P_1 - P_2) 2\pi h dh = dF = 2\ 2\pi h \ell \mu \frac{\partial^2 v}{\partial h^2} dh.$$

Or,

$$\frac{P_1 - P_2}{\ell} = - \mu \frac{\partial^2 v}{\partial h^2}.$$

In the limit as ℓ approaches zero, $\frac{P_1 - P_2}{\ell}$ becomes $\frac{dP}{dx}$ and

$$\frac{dP}{dx} = -\mu \frac{\partial^2 v}{\partial h^2}.$$

More generally,

$$\frac{dP}{dx} = - \mu \nabla_r^2 v \tag{1A}$$

where ∇_r^2 is the radial Laplacian operator in the coordinate system being used.

An elliptical tube is shown below.

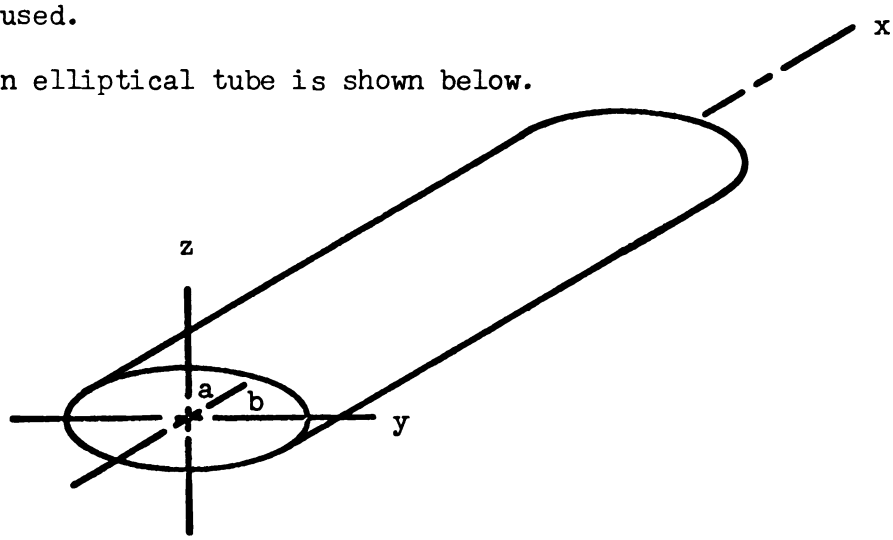

For this case (1A) becomes

$$\frac{dP}{dx} = - \mu \left(\frac{\partial^2 v}{\partial z^2} + \frac{\partial^2 v}{\partial y^2} \right). \tag{1B}$$

This equation has the solution

$$v = c\left(1 - \frac{z^2}{a^2} - \frac{y^2}{b^2}\right),$$

providing

$$c = \frac{1}{2u} \frac{a^2 b^2}{a^2 + b^2} \frac{dP}{dx} .$$

Therefore,

$$v = \frac{1}{2u} \frac{a^2 b^2}{a^2 + b^2} \frac{dP}{dx}\left(1 - \frac{z^2}{a^2} - \frac{y^2}{b^2}\right)$$

The volume flow rate (Q) is

$$Q = \int_0^b \int_0^b v \, dy \, dz = \frac{dP}{dx} \frac{\pi}{4u} \frac{a^3 b^3}{a^2 + b^2} .$$

Since the resistance per unit length is defined to be the pressure drop divided by the volume flow rate,

$$r = \frac{dP}{dx}/Q = \frac{4u}{\pi} \frac{a^2 + b^2}{a^3 b^3} .$$

For a tube of constant perimeter "$a^2 + b^2$" is nearly a constant, hence, combining the constant terms

$$r = K'/a^3 b^3$$

For an ellipse, $a^3 b^3 = A^3/\pi^3$, and therefore,

$$r = K/A^3 \quad \text{where} \quad K = 4u\,(a^2 + b^2)\pi^2$$

This leads directly to the required result,

$$r A^3 = r'(A')^3 \quad \text{or,} \quad r = \frac{r'(A')^3}{A^3}$$ which is used in the theoretical development.

Appendix B

The computer program logic and programs for solving the open loop, closed loop, and pressure distributions are presented in this section. Each program is followed by a table of the results which are used in the body of the thesis. The logic proceeds as follows:

1. Set P_c and R_s.
2. Guess a value of Q.
3. Check to be sure Q is not too large.
4. Use a third-order Runge-Kutta technique to step along the tube increments of Δx from $x = 0$ to $x = \ell$.
5. Check to see if the value of Q meets the end boundary condition.
6. If it does, print out results, index the applied pressure and use the current value of Q for the next operation at the new value of P_c.
7. If the end boundary condition is not satisfied, check to see if cycle has been performed more than once.
8. If this is the first guess at Q, check the sign of the error at the end boundary condition and guess at a new value of Q accordingly.
9. See if the error has changed in sign if the cycle has been performed more than once.
10. If the error has changed in sign, Q is somewhere between the old value and the present value so start searching between these two points.
11. If the error has not changed in sign, guess at a new value of Q ac-

cordingly. The final search routine consists of a simple interval slicing technique.

The parametric fluid flow control curves predicted by the computer program are shown in Fig. 6. The results plotted are for a x = 0.5 cm for a 30 cm tube length. When x was reduced to 0.25 cm, the values of flow changed a maximum of 0.05% showing that the procedure of lumping the tube into 0.5 cm lengths is sufficient and this value was used thereafter.

The same area subroutine listed below was used for each program.

```
      SUBROUTINE AREA (C,A,DA)
      IF(C-15.)10,10,125
   10 CA=C*C*.159
      CB=C*C*.0061
      A=.362/EXP(CA) +.105/EXP(CB) +.0398/(C+1.)**.2 +.03
      DA=.115*C/EXP(CA) +.00128*C/EXP(CB) +.00796/(C+1.)**1.2
      GO TO 600
  125 IF(C-50.)201,201,24
  201 CB=C*C*.0061
      A=.105/EXP(CB) +.0398/(C+1.)**.2 +.03
      DA=.00128*C/EXP(CB) +.00796/(C+1.)**1.2
      GO TO 600
   24 A=.0398/(C+1.)**.2 +.03
      DA=.00796/(C+1.)**1.2
  600 RETURN
      END
```

Listed below is the computer program used to solve the closed loop curves.

```
25      READ(5,100) R,DX,H,NO
100     FORMAT(3E16.8,I10)
        WRITE(6,103) R,DX,NO
103     FORMAT(1H1,7X,16HSOLUTION FOR R =,F5.2,8H,  DX = ,F4.2,7H,
        NO =, I15)
        Q=2.66
        PC=1.
        DO 1 K=1,20
        IO=0
805     I=0
        N=0
        IF(IO-50)3,3,11
 3      PA=PC-Q*R
        E=Q*DX*.000155
        F=Q*Q*.00102
        IF(PA)4,4,5
  4     Q=Q-.1
        GO TO 3
5       DO 6 L=1,NO
        C=PC-PA
        CALL AREA (C,A,DA)
        DENO=A**3-F*DA
        IF(DENO)804,804,801
801     RKA=-E/DENO
        PAG=PA+.5*RKA
        C=PC-PAG
        CALL AREA (C,A,DA)
        DENO=A**3-F*DA
        IF(DENO)804,804,802
804     IO=IO+1
        Q=Q-.051
        GO TO 805
802     RKB=-E/DENO
        PAG=PA+2.*RKB-RKA
        C=PC-PAG
        CALL AREA (C,A,DA)
        DENO=A**3-F*DA
        IF(DENO)804,804,803
803     RKC=-E/DENO
 6      PA=PA+(RKA+4.*RKB+RKC)/6.
        N=N+1
        IF(N-75)505,505,11
505     C=ABS(PC-PA)
```

```
      CALL AREA (C,A,DA)
502   PA=PA-4.*F+2.*F/A
      IF(ABS(PA)-H)11,11,12
  12  IF(N-1)17,17,14
  17  IF(PA)15,15,16
  15  QB=Q
      PAB=PA
      Q=Q-.05
      GO TO 3
  16  QB=Q
      PAB=PA
      Q=Q+.05

      GO TO 3
  14  IF(PA*PAB)18,13,13
  13  IF(I)17,17,20
  18  I=I+1
      QA=Q
      PAA=PA
      GO TO 19
  20  QB=Q
      PAB=PA
  19  Q=QB+.3*(QA-QB)
      IF(ABS(QA-QB)-.001)11,11,3
 11   WRITE(6,102) PC,N,Q
102   FORMAT(1H0,4X,4HPC =,F5.1,11X,3HN =,I3,13X,3HQ =,F9.5)
      IF(PC-9.)700,700,701
700   PC=PC+1.
      GO TO 1
701   PC=PC+6.
 1    CONTINUE
      IF(R-10.)25,25,26
  26  STOP
      END
```

Tabulated Results of Computer
Solution for Closed Loop Operation

Series Resistance	5.0	2.0	1.0	0.7	0.6	0.5	0.4	0.3	0.2
$P_1 = P_c$(cm-H_2O)									
2	0.36	0.96	1.82	2.52	2.91	3.41	4.11	5.26	7.21
4	0.71	1.58	2.78	3.66	4.10	4.69	5.48	6.63	8.46
6	0.94	1.91	3.16	4.04	4.48	5.05	5.83	6.95	8.72
8	1.16	2.22	3.46	4.32	4.75	5.32	6.07	7.17	8.90
10	1.35	2.48	3.71	4.54	4.96	5.50	6.24	7.30	8.99
16	1.65	2.87	4.07	4.84	5.23	5.73	6.43	7.44	9.04
22	1.76	3.00	4.19	4.94	5.31	5.81	6.48	7.47	Unstable
34	1.88	3.15	4.34	5.07	5.43	5.91	6.57	7.55	
46	2.00	3.29	4.48	5.20	5.55	6.02	6.67	7.63	
58	2.11	3.42	4.62	5.32	5.66	6.12	6.76	7.71	
70	2.23	3.54	4.75	5.44	5.78	6 22	6.85	7.78	

Resulting Flow Rate (cm^3/sec)

Listed below is the computer program used to solve for the open loop curves. The logic of the program is basically the same as that used for the closed loop curves except that the boundary condition at x = 0 is independently controlled.

```
25      READ(5,100) R,DX,H,NO
100     FORMAT(3E16.8,I10)
        PC=10.
        DO 1 K=1,7
        Q=.001
        PAK=1.
        WRITE(6,103) PC
103     FORMAT(1H1,7X,26HOPEN LOOP SOLUTION FOR PC=,F5.2)
        IC=0
805     I=0
        N=0
        IF(IO-50)3,3,11
3       PA=PAK
        E=Q*DX*.000155
        F=Q*Q*.00102
5       DO 6 L=1,NO
        C=ABS(PC-PA)
        CALL AREA (C,A,DA)
        DENO=A**3-F*DA
        IF(DENO)804,804,801
801     RKA=-E/DENO
        PAG=PA+.5*RKA
        C=ABS(PC-PAG)
        CALL AREA (C,A,DA)
        DENO=A**3-F*DA
        IF(DENO)804,804,802
804     IC=IO+1
        Q=Q-.051
        GO TO 805
802     RKB=-E/DENO
        PAG=PA+2.*RKB-RKA
        C=ABS(PC-PAG)
        CALL AREA (C,A,DA)
        DENO=A**3-F*DA
        IF(DENO)804,804,803
803     RKC=-E/DENO
 6      PA=PA+(RKA+4.*RKB+RKC)/6.
        N=N+1
        IF(N-75)505,505,11
505     C=ABS(PC-PA)
        CALL AREA (C,A,DA)
502     PA=PA-4.*F+2.*F/A
        IF(ABS(PA)-H)11,11,12
  12    IF(N-1)17,17,14
  17    IF(PA)15,15,16
  15    QB=Q
```

```
      PAB=PA
      Q=Q-.05
      GO TO 3
16    QB=Q
      PAB=PA
      Q=Q+.05
      GO TO 3
14    IF(PA*PAB)18,13,13
13    IF(I)17,17,20
  18  I=I+1
      QA=Q
      PAA=PA
      GC TO 19
  20  QB=Q
      PAB=PA
  19  Q=QB+.3*(QA-QB)
      IF(ABS(QA-QB)-.001)11,11,3
11    WRITE(6,102) PAK,N,Q
102   FORMAT(1HO,4X,4H P =,F5.1,11X,3HN =,I3,13X,3HQ =,F9.5)
      PAK=PAK+1.
      IF(PAK-PC)805,805,701
701   PC=PC+10.
 1    CONTINUE
      IF(R-10.)25,25,26
  26  STOP
      END
```

Tabulated Results of
Computer Solution
for Open Loop Operation

P_c(cm-H_2O)	P_2(cm-H_2O)	Q(cm^3/sec)	P_c(cm-H_2O)	P_2(cm-H_2O)	Q(cm^3/sec)
10	1	0.33	40	36	4.74
10	2	0.73	40	37	5.94
10	3	1.21	40	38	8.51
10	4	1.77			
10	5	2.44	50	20	0.51
10	6	3.34	50	30	0.85
10	7	4.91	50	35	1.20
10	8	8.08	50	40	2.09
10	9	11.83	50	42	2.75
			50	44	3.66
20	5	0.36	50	45	4.22
20	8	0.80	50	46	4.93
20	10	1.28	50	47	6.09
20	12	1.98	50	48	8.59
20	14	2.93			
20	15	3.53	60	25	0.61
20	16	4.30	60	35	0.89
20	17	5.59	60	40	1.08
20	18	8.30	60	45	1.43
			60	50	2.31
			60	52	2.97
30	10	0.34	60	52	2.97
30	15	0.70	60	54	3.86
30	20	1.60	60	55	4.41
30	22	2.29	60	56	5.11
30	24	3.22	60	57	6.24
30	25	3.80	60	58	8.72
30	26	4.54			
30	27	5.77	70	35	0.84
30	28	8.38	70	45	1.12
			70	50	1.30
40	15	0.41	70	55	1.65
40	20	0.60	70	60	2.52
40	25	0.96	70	62	3.17
40	30	1.85	70	64	4.05
40	32	2.53	70	65	4.60
40	34	3.45	70	66	5.28
40	35	4.02	70	67	6.39
			70	68	8.80

The computer program used to solve for the pressure distributions is listed below. The flow rate solutions obtained from the closed loop program are used in this program.

```
25    READ(5,100)R,PC,Q
100   FORMAT(3E16.8)
      WRITE(6,103)R,PC,Q
103   FORMAT(1H1,7X,29HPRESSURE DISTRIBUTION FOR R =,F5.2,8H,  PC =
     1F6.2,7H,   Q =,F9.5)
      WRITE(6,104)
104   FORMAT(1H ,10X,1HX,15X,1HP)
      X=.0
      E=Q*.0000775
      F=Q*Q*.001C2
      PA=PC-Q*R
5     DO 6 L=1,60
      WRITE(6,105) X,PA
105   FORMAT(1H ,7X,F5.2,10X,F12.5)
      C=ABS(PC-PA)
      CALL AREA (C,A,DA)
      DENO=A**3-F*DA
801   RKA=-E/DENO
      PAG=PA+.5*RKA
      C=ABS(PC-PAG)
      CALL AREA (C,A,DA)
      DENO=A**3-F*DA
802   RKB=-E/DENO
      PAG=PA+2.*RKB-RKA
      C=ABS(PC-PAG)
      CALL AREA (C,A,DA)
      DENO=A**3-F*DA
803   RKC=-E/DENO
      X=X+.5
 6    PA=PA+(RKA+4.*RKB+RKC)/6.
      IF(R-10.)25,25,26
 26   STOP
      END
```

Computer Results for
Pressure Distribution for $R_s = 5.0$
and Values of $P_c = P_1$ (cm-H_2O)

Distance x cm	$P_c = 10$	$P_c = 16$	$P_c = 22$	$P_c = 34$	$P_c = 52$
0.0	3.27	7.77	13.22	24.59	41.72
4.0	2.93	7.22	12.55	23.76	40.60
8.0	2.56	6.60	11.78	22.77	39.15
12.0	2.18	5.89	10.87	21.52	37.04
16.0	1.76	5.07	9.74	19.81	33.44
20.0	1.31	4.07	8.26	17.18	26.47
22.0	1.07	3.48	7.31	15.20	21.68
24.0	0.82	2.81	6.13	12.47	16.50
25.0	0.69	2.43	5.42	10.77	13.83
26.0	0.56	2.02	4.61	8.86	11.11
27.0	0.42	1.58	3.68	6.77	8.34
28.0	0.28	1.09	2.60	4.55	5.54
29.0	0.13	0.55	1.34	2.24	2.70
29.5	0.06	0.25	0.64	1.06	1.27

Computer Results for
Pressure Distribution for P_c = 16 (cm-H_2O)
and Values of R_s

Distance x cm	R_s = 5.0	R_s = 2.0	R_s = 1.0	R_s = 0.5	R_s = 0.2
0.0	7.77	10.26	11.93	13.13	14.19
4.0	7.22	9.62	11.36	12.83	14.05
8.0	6.60	8.90	10.62	12.37	13.89
12.0	5.89	8.08	9.73	11.63	13.66
16.0	5.07	7.10	8.67	10.53	13.33
20.0	4.07	5.90	7.35	9.12	12.60
22.0	3.48	5.16	6.54	8.25	11.64
24.0	2.81	4.29	5.55	7.19	10.41
25.0	2.43	3.78	4.97	6.56	9.76
26.0	2.02	3.21	4.30	5.81	9.03
27.0	1.58	2.56	3.50	4.91	8.17
28.0	1.09	1.80	2.53	3.74	7.07
29.0	0.55	0.90	1.29	2.07	5.42
29.5	0.25	0.38	0.51	0.87	3.98

Appendix C

Experimental Data from Hydraulic Test Section

Area as a Function of Pressure

Applied Pressure ($cm-H_2O$)	Displaced Vol (cm^3)	Resulting Change in Area (cm^2)	Area (cm^2)
0.0	0.0	0.0	0.537
1.0	0.8	0.027	0.510
1.5	1.6	0.053	0.484
2.0	4.2	0.140	0.397
2.2	6.0	0.200	0.337
2.5	8.0	0.267	0.270
2.8	9.0	0.300	0.237
3.2	9.9	0.330	0.207
4.0	10.8	0.360	0.177
4.9	11.2	0.374	0.163
10.0	12.8	0.427	0.110
18.0	14.0	0.467	0.070
27.0	14.5	0.484	0.053
40.0	14.8	0.494	0.043
Above 100	15.2	0.507	*0.030

*Assumed for the case when the tube is completely collapsed.

Data for Open Loop Curves

P_c = 70 cm-H_2O

P_2 cm-H_2O	P_3 cm-H_2O	ΔP cm-H_2O	Q cm^3/sec
26.2	1.0	25.2	0.44
31.0	1.0	30.0	0.57
41.3	1.2	40.1	0.93
51.6	1.3	50.3	1.51
62.0	1.3	60.7	2.56
65.0	1.4	63.6	3.28
67.0	1.4	65.6	3.80
68.0	1.4	66.6	4.71
68.6	1.5	67.1	6.42
69.0	1.5	67.5	7.58
69.2	1.5	Unstable	

P_c = 60 cm-H_2O

P_2 cm-H_2O	P_3 cm-H_2O	ΔP cm-H_2O	Q cm^3/sec
55.8	1.4	54.4	3.61
56.6	1.4	55.2	3.92
57.7	1.4	56.3	4.42
58.5	1.4	57.1	5.52
58.8	1.4	57.4	7.25
42.6	1.2	41.4	1.67
48.5	1.2	47.3	2.22
34.0	1.1	32.9	1.11
24.5	1.1	23.4	0.67
15.0	1.1	13.9	0.33
59.0	1.5	Unstable	

P_c = 50 cm-H_2O

P_2 cm-H_2O	P_3 cm-H_2O	ΔP cm-H_2O	Q cm^3/sec
15.0	1.1	13.9	0.44
22.0	1.1	20.9	0.76
30.3	1.2	29.1	1.33
36.5	1.2	35.3	1.75
43.0	1.3	41.7	2.77
47.0	1.4	45.6	4.23
48.7	1.4	47.3	7.43
49.0	1.5	Unstable	

P_c = 40 cm-H_2O

P_2 cm-H_2O	P_3 cm-H_2O	ΔP cm-H_2O	Q cm^3/sec
38.3	1.5	36.8	6.74
38.5	1.5	37.0	7.82
39.0	1.5	37.5	9.33
37.0	1.5	35.5	4.92
35.1	1.4	33.7	3.87
33.8	1.4	32.4	3.36
29.0	1.3	27.7	2.38
24.2	1.3	22.9	1.75
19.0	1.2	17.8	1.11
12.5	1.2	11.3	0.58
6.3	1.1	5.2	0.23
39.1	Unstable		

P_c = 30 cm-H_2O

P_2 cm-H_2O	P_3 cm-H_2O	ΔP cm-H_2O	Q cm^3/sec
6.0	1.2	4.8	0.33
12.0	1.3	11.7	0.90
20.0	1.3	18.7	2.17
25.0	1.4	23.6	3.20
27.5	1.4	26.1	4.52
28.5	1.5	27.0	6.69
29.0	1.5	27.5	9.03
29.1	Unstable		

P_c = 20 cm-H_2O

P_2 cm-H_2O	P^3 cm-H_2O	ΔP cm-H_2O	Q cm^3/sec
5.5	1.3	4.2	1.0
13.0	1.3	11.7	2.50
14.2	1.4	12.8	3.13
17.3	1.4	15.9	4.67
17.7	1.5	16.2	5.06
18.4	1.5	16.9	9.33
18.6	Unstable		

P_c = 10 cm-H_2O

P_2 cm-H_2O	P_3 cm-H_2O	ΔP cm-H_2O	Q cm^3/sec
3.1	1.3	1.8	0.70
3.7	1.3	2.4	1.59
6.8	1.4	5.4	3.87
8.5	1.5	7.0	8.90
8.0	1.4	6.6	8.38

Data for Closed Loop Curves

R_s = 4.5

$P_1 = P_c$ cm-H_2O	P_2 cm-H_2O	P_3 cm-H_2O	$\Delta P = P_1 - P_3$	Q cm^3/sec
4.5	2.2	1.7	2.8	.772
8.0	3.5	1.8	6.2	1.25
16.0	8.3	1.8	14.2	1.79
25.6	16.1	1.8	24.8	2.10
42.1	31.5	1.8	40.3	2.32
58.5	47.2	1.8	56.7	2.39
78.5	67.0	1.8	76.7	2.44

R_s = 0.73

$P_1 = P_c$ cm-H_2O	P_2 cm-H_2O	P_3 cm-H_2O	$\Delta P = P_1 - P_3$ cm-H_2O	Q cm^3/sec
3.5	2.2	1.8	1.7	2.76
6.6	4.4	1.8	4.8	3.50
14.7	11.8	1.8	12.9	4.13
27.2	24.0	1.8	25.4	4.36
41.5	38.3	1.8	39.7	4.37
56.6	53.5	1.8	80.6	4.30

R_s = 0.40

$P_1 = P_c$ cm-H_2O	P_2 cm-H_2O	P_3 cm-H_2O	$\Delta P = P_1 - P_3$ cm-H_2O	Q cm^3/sec
84.8	84.8	84.8	0	0
83.3	81.2	1.8	81.5	5.21
76.4	74.4	1.8	74.6	5.21
66.6	64.5	1.8	64.8	5.18
50.0	47.9	1.8	48.2	5.21
35.9	33.8	1.8	28.8	5.12
21.0	19.0	1.8	16.3	4.99
13.0	11.0	1.8	11.2	4.83
6.9	5.0	1.8	5.1	4.48
3.5	2.0	1.8	1.7	1.54

R_s = 0.28

$P_1 = P_c$ cm-H_2O	P_2 cm-H_2O	P_3 cm-H_2O	$\Delta P = P_1 - P_3$ cm-H_2O	Q cm^3/sec
27.8	26.0	1.8	26.0	6.23
16.8	15.1	1.8	15.0	6.06
11.6	9.1	1.8	9.8	5.92
6.8	5.2	1.8	5.0	5.70
4.0	2.5	1.8	2.2	5.62
4.7	3.2	1.8	2.9	5.79
7.6	6.0	1.8	5.8	5.86
11.1	9.5	1.8	9.3	6.05
16.6	14.9	1.8	14.8	6.12
22.6	20.8	1.8	20.8	6.16
31.5	29.8	1.8	29.7	6.16
37.8	36.1	1.8	36.0	6.16
52.5	50.8	1.8	50.7	6.12
83.4	81.4	1.8	81.6	6.02

R_s = 0.21

$P_1 = P_c$ cm-H_2O	P_2 cm-H_2O	P_3 cm-H_2O	$\Delta P = P_1 - P_3$ cm-H_2O	Q cm^3/sec
3.5	2.0	1.8	1.7	7.12
5.6	4.1	1.8	3.8	7.42
7.1	5.6	1.8	5.3	7.32
9.8	8.2	1.8	8.0	7.32
9.8	8.2	1.8	8.0	7.28
12.9	11.3	1.8	11.1	7.23
9.5	8.0	1.8	7.7	7.18
14.2	12.7	1.8	12.4	7.18
19.0	17.5	1.8	17.2	7.18
28.0	26.5	1.8	26.2	7.13
40.1	38.5	1.8	38.3	7.08
40.1	38.6	1.8	38.3	7.03
53.4	52.0	1.8	51.6	6.97
64.1	62.7	1.8	62.3	6.95
85.0	83.6	1.8	83.2	6.90

Appendix D

Experimental Data from Dog Kidneys

	P_a	P_{DV}	$P_a - P_{DV}$	Q
Kidney I	8	1	7	0.17
	30	6	24	0.75
	58	8	50	1.90
	72	10	62	2.16
	93	12	81	2.70
	120	19	101	2.83
	132	25	107	2.95
Kidney II	8	1	7	0.25
	31	7	24	1.55
	62	15	47	2.59
	83	20	63	4.05
	108	29	79	5.00
	126	43	83	5.27
	139	47	92	5.42
	146	55	91	5.58
Kidney III	9	2	7	-
	25	7	18	0.34
	34	8	26	0.50
	52	13	39	0.92
	61	14	47	1.05
	78	20	58	1.28
	90	26	64	1.70
	103	27	76	1.72
	114	33	81	1.88
	123	36	87	1.88
	131	40	91	1.82
	139	46	93	1.95
Kidney IV	29	3	26	0.50
	52	4	48	1.08
	62	5	57	1.33
	77	6	71	1.83
	86	7	79	1.92
	99	9	90	2.25
	107	11	96	2.33
	124	16	108	2.50
	138	24	114	2.62

	P_a	P_{DV}	$P_a - P_{Dv}$	Q
Kidney V	15	2	13	0.16
	36	9	27	0.75
	64	17	47	1.37
	97	29	68	2.15
	115	38	77	2.33
	123	46	77	2.45
	137	52	85	2.55
	144	56	88	2.60
Kidney VI	35	4	31	1.2
	54	6	48	1.94
	68	10	58	2.40
	84	13	71	3.02
	97	21	76	3.20
	112	28	84	3.47
	125	33	92	3.56
	134	38	96	3.66
Kidney VII	42	3	39	0.58
	51	4	47	0.73
	68	7	61	1.17
	81	11	70	1.42
	93	14	79	1.33
	100	20	80	1.67
	111	26	85	1.73
	124	30	94	1.67
	132	32	100	1.80
	140	36	104	1.78
	148	41	107	1.85
Kidney VIII	22	8	14	0.22
	32	11	21	0.52
	44	11	33	0.95
	52	12	40	1.08
	60	15	45	1.34
	71	20	51	1.79
	85	23	62	2.34
	94	28	66	2.50
	102	31	71	2.74
	116	33	83	2.75
	123	35	88	2.84
	135	37	98	2.77
	144	44	100	2.84